



Photoproduction of low- p_T J/ψ from peripheral to central Pb–Pb collisions at 5.02 TeV

ALICE Collaboration*

ARTICLE INFO

Article history:

Received 25 May 2022

Received in revised form 18 August 2022

Accepted 22 September 2022

Available online 17 September 2023

Editor: M. Pierini

ABSTRACT

An excess of J/ψ yield at very low transverse momentum ($p_T < 0.3$ GeV/c), originating from coherent photoproduction, is observed in peripheral and semicentral hadronic Pb–Pb collisions at a center-of-mass energy per nucleon pair of $\sqrt{s_{NN}} = 5.02$ TeV. The measurement is performed with the ALICE detector via the dimuon decay channel at forward rapidity ($2.5 < y < 4$). The nuclear modification factor at very low p_T and the coherent photoproduction cross section are measured as a function of centrality down to the 10% most central collisions. These results extend the previous study at $\sqrt{s_{NN}} = 2.76$ TeV, confirming the clear excess over hadronic production in the p_T range $0 – 0.3$ GeV/c and the centrality range 70–90%, and establishing an excess with a significance greater than 5σ also in the 50–70% and 30–50% centrality ranges. The results are compared with earlier measurements at $\sqrt{s_{NN}} = 2.76$ TeV and with different theoretical predictions aiming at describing how coherent photoproduction occurs in hadronic interactions with nuclear overlap.

© 2022 The Author(s). Published by Elsevier B.V. This is an open access article under the CC BY license (<http://creativecommons.org/licenses/by/4.0/>). Funded by SCOAP³.

Diffractive photoproduction of J/ψ mesons in nucleus–nucleus collisions is sensitive to the nuclear gluon distributions at low Bjorken- x , in the range $x \sim 10^{-5}$ to 10^{-2} at LHC energies, where they are still poorly constrained [1–3]. This process was extensively studied in nuclear collisions with impact parameters larger than twice the nuclear radius, known as ultra-peripheral collisions (UPCs) [4–9]. In UPCs, hadronic interactions are strongly suppressed providing a clean experimental environment to study photon-induced processes.

Photonuclear reactions are produced by the strong electromagnetic field generated by ultra-relativistic ions, which can be treated as a flux of quasi-real photons. At leading order in perturbative quantum chromodynamics (pQCD), the photon fluctuates into a quark–antiquark pair (a color dipole) [10], which probes the gluon distribution of the target via the exchange of two gluons in a singlet color state, with the dipole finally recombining into a vector meson (VM) [11,12]. The diffractive VM photoproduction on nuclei can be either coherent or incoherent. In the coherent interaction, the photon couples with the nucleus as a whole, leaving it intact. The produced VM is characterized by a very low average transverse momentum ($\langle p_T \rangle \approx 60$ MeV/c). In incoherent photoproduction the photon couples to a single nucleon which leads to the breakup of the nucleus. In this case a VM with larger average transverse momentum ($\langle p_T \rangle \approx 500$ MeV/c) is produced.

In nuclear collisions with impact parameters smaller than the sum of the radii of the colliding nuclei, production from hadronic interactions becomes the dominant contribution to the J/ψ yield. Hadroproduction of J/ψ mesons in Pb–Pb collisions is a long-standing probe of the quark-gluon plasma (QGP), a state of strongly-interacting matter characterized by quark and gluon degrees of freedom predicted by QCD to exist at high temperature and energy density. Charmonium production is affected by the QGP, and their measured yields [13–16] are explained as an interplay between suppression due to color screening [17] and recombination of charm quarks [18–20]. Finally, the charmonium yield can also be influenced by cold nuclear matter effects (CNM), which can be studied independently in p–Pb collisions [21–24].

The ALICE Collaboration reported the presence of an unexpectedly large J/ψ yield at very low p_T in peripheral Pb–Pb collisions at a center-of-mass energy per nucleon pair of $\sqrt{s_{NN}} = 2.76$ TeV [25], which could not be explained by any combination of suppression, regeneration, and CNM effects [26]. Coherent photoproduction of J/ψ in Pb–Pb collisions with nuclear overlap was proposed as a plausible mechanism to explain this observation [25]. A similar low- p_T J/ψ excess was later measured by the STAR Collaboration at RHIC in Au–Au collisions at $\sqrt{s_{NN}} = 200$ GeV and U–U collisions at $\sqrt{s_{NN}} = 193$ GeV [27]. The STAR measurement of the t -dependence (Mandelstam variable, $t \approx -p_T^2$ for large $\sqrt{s_{NN}}$) of the excess showed a strong similarity with the one measured in UPCs, also pointing to coherent photoproduction as the origin of the excess. Similar conclusions can be drawn from the recent measurement of the J/ψ yields at low p_T in Pb–Pb collisions

* E-mail address: alice-publications@cern.ch.

at $\sqrt{s_{\text{NN}}} = 5.02$ TeV by the LHCb Collaboration [28]. In addition, dilepton pairs with characteristics compatible with photoproduction were observed in non-UPC heavy-ion collisions by the ATLAS, STAR, and ALICE experiments [29–31].

The concept of coherent photoproduction in a hadronic environment raises several theoretical challenges. For example, how can the coherence condition survive in the photon–nucleus interaction if the latter is broken up during the hadronic collision? Do only the (non-interacting) spectator nucleons participate in the coherent process? To what extent is the photon–nucleus cross section modified by target nucleons undergoing hadronic interactions and losing energy before the photoproduction occurs? How is the yield of the photoproduced J/ψ mesons, characterized by low transverse momenta, affected by interactions with the formed and fast-expanding QGP medium? The measurements mentioned above triggered novel theoretical developments [26,32–36] based on calculations for UPCs in which the nuclear photoproduction cross section of a VM is usually computed as the product of a quasi-real photon flux with the photon–nucleus cross section corresponding to the $\gamma A \rightarrow \text{VM} + A$ interaction, where γ is the photon and A is the nucleus. For collisions with nuclear overlap, in all considered models, an effective photon flux is introduced to take into account the geometrical constraints of a given impact-parameter range. Depending on the model, the photon–nucleus cross section is sometimes also modified to account for the effective size of nuclear fragments participating in the coherent process [32,34]. Calculations from Ref. [34] highlight the interest of measuring the cross section (and additionally its transverse momentum dependence) of the J/ψ excess towards more central collisions in order to probe possible changes of the effective size of the coherently interacting volume. Additionally, it was suggested that the measurement of the J/ψ coherent photoproduction in UPCs and in peripheral collisions in the same rapidity range at forward rapidity can be used to extract the coherent photon–nucleus cross section in two different Bjorken- x regions, below 10^{-4} and above 10^{-2} at LHC energies [37].

In this Letter, the measurement of the J/ψ nuclear modification factor and the coherent photoproduction at low p_T at forward rapidity in Pb–Pb collisions at $\sqrt{s_{\text{NN}}} = 5.02$ TeV are presented as a function of collision centrality. The measurement uses a pp reference at the same energy that is described in Ref. [38]. The larger data set compared to the one at $\sqrt{s_{\text{NN}}} = 2.76$ TeV [25] allows for the first time the observation of a significant excess in the 50–70% and 30–50% centrality intervals. Assuming that the observed excess originates from coherent J/ψ photoproduction, the corresponding cross section is extracted as a function of the collision centrality. For centrality intervals where no significant excess could be measured, an upper limit on the cross section is reported.

The ALICE detector and its performance are described in detail in Refs. [39,40]. In this analysis, the J/ψ production is measured at forward rapidity ($2.5 < y < 4$) and down to $p_T = 0$ in the dimuon decay channel with the forward muon spectrometer, consisting of a tracking system placed downstream of a front absorber of composite material, and a trigger system placed downstream of a muon filter made of iron. The interaction vertex is determined with the Silicon Pixel Detector (SPD), which consists of the two innermost layers of the Inner Tracking System in the central barrel. The first and second innermost layers cover the pseudorapidity ranges $|\eta| < 2$ and $|\eta| < 1.4$, respectively. The V0 detector, consisting of two scintillator hodoscopes placed on both sides of the interaction point and covering the pseudorapidity range $2.8 < \eta < 5.1$ and $-3.7 < \eta < -1.7$, is used for triggering, beam–gas background rejection and determination of the collision centrality, which is evaluated by fitting the signal amplitude distribution in the V0 as described in Ref. [41]. The Zero Degree Calorimeters (ZDCs) are placed on both sides of the interaction point along the beam

direction at a distance of 112.5 m from it and measure the spectator protons and neutrons. The requirement of a minimum energy deposited in the two neutron calorimeters, corresponding to the expected signal from one spectator neutron, and the combined use of the V0 and ZDC timing information, suppresses the background induced by electromagnetic dissociation processes [42].

The data sample considered in this analysis, collected in 2015 and 2018, consists of events where two opposite sign muons are detected in the trigger system of the muon spectrometer, each with a p_T above the trigger threshold of 1 GeV/c, in coincidence with a minimum-bias (MB) trigger. The latter is defined by the coincidence of a signal in both arrays of the V0 detector. Events are selected in the 0–90% centrality interval, where the MB trigger is fully efficient. The data sample used for this analysis amounts to 4×10^8 triggered Pb–Pb collisions, corresponding to an integrated luminosity of $756 \pm 19 \mu\text{b}^{-1}$ [43], where the uncertainty is systematic (the statistical one being negligible).

J/ψ candidates are formed by combining pairs of opposite-sign (OS) muon tracks reconstructed in the geometrical acceptance of the muon spectrometer ($-4 < \eta < -2.5$). The muon identification is ensured by requiring that each track reconstructed in the tracking chambers matches a track segment in the trigger system. The single-muon and dimuon selection criteria are the same as the ones used in previous analyses [14,25]. The raw number of J/ψ is extracted in five centrality classes (0–10%, 10–30%, 30–50%, 50–70% and 70–90%) and two p_T ranges with the aim to study the coherent (0–0.3 GeV/c) and the incoherent photoproduction (0.3–1 GeV/c). The choice of the transverse momentum intervals takes into account the broadening of the reconstructed transverse momentum distribution of coherently and incoherently photoproduced J/ψ , mainly due to multiple scattering in the front absorber. The raw yield is also extracted in eight p_T intervals up to 8 GeV/c in order to estimate the hadronic contribution as explained below. The signal extraction is performed by fitting the invariant mass distribution of the OS dimuons using various combinations of functional forms for the signal and background shapes as discussed in the following. The raw J/ψ yield and its statistical uncertainty is then determined as the average of all obtained yield values and corresponding statistical uncertainties, respectively, while the associated systematic uncertainty is taken as the standard deviation of the results. The signal is modeled through an extended Crystal Ball function or a pseudo-Gaussian with a mass-dependent width [44]. The non-Gaussian tails were fixed to the values obtained by fitting either a large sample in pp collisions at $\sqrt{s} = 13$ TeV [45] or MC simulations where the hadroproduced J/ψ signal is embedded into real events in order to account for detector occupancy effects. In the p_T ranges 0–0.3 GeV/c and 0.3–1 GeV/c, additional sets of tails are obtained from MC simulations that use as input coherently and incoherently photoproduced J/ψ from the STARlight MC generator [46]. The underlying continuum is described with either a variable-width Gaussian or the ratio of second and third order polynomials [44,47].

The nuclear modification factor in the centrality interval i is defined as

$$R_{\text{AA}}^i(p_T) = \frac{N_{J/\psi}^i(p_T)}{\text{BR}_{J/\psi \rightarrow \mu^+ \mu^-} \times N_{\text{MB}}^i \times A\varepsilon^{i,h}(p_T) \times \langle T_{\text{AA}}^i \rangle \times \sigma_{\text{pp}}(p_T)}, \quad (1)$$

where $N_{J/\psi}^i$ are the measured raw yields, $A\varepsilon^{i,h}$ is the detector acceptance and efficiency (assuming unpolarized hadroproduction), $\text{BR}_{J/\psi \rightarrow \mu^+ \mu^-}$ is the branching ratio to muon pairs [48], N_{MB}^i is the equivalent number of MB events, $\langle T_{\text{AA}}^i \rangle$ is the average nuclear overlap function, and σ_{pp} is the measured J/ψ cross section in pp collisions at the same center-of-mass energy [38].

Table 1

Systematic uncertainties (in percent) on the R_{AA} measurement for different J/ψ p_T intervals. Ranges correspond to the range of values in different centrality classes, whereas the values marked with an asterisk are independent of centrality.

p_T	0–0.3 GeV/c	0.3–1 GeV/c	1–2 GeV/c
Signal extraction	1.8–3.7	1.5–3.4	2.4–3.4
MC input		2.5	
Tracking eff.		0–1 + 3*	
Trigger eff.	0–1 + 2.8*	0–1 + 2.0*	0–1 + 1.5*
Matching eff.		1*	
N_{MB}		0.3*	
$\langle T_{AA} \rangle$		0.7–2.4	
Centrality limits		0.2–7	
pp cross section	5.8*	5.4*	5.1*

The $A\varepsilon$ values are estimated with MC simulations where the J/ψ input p_T and y distributions are adjusted to data, and separately tuned for each centrality class using an iterative procedure. The time-dependent status of the electronics channels for the tracking chambers, as well as misalignment of the detector elements, were taken into account. The efficiency of the trigger chambers was determined from data and used in the simulations. The systematic uncertainty on the $A\varepsilon$ value derives from the uncertainty on the MC input p_T and y distributions and on the tracking, trigger and matching efficiency. The former was evaluated by varying the input shapes tuned on data within the statistical uncertainty and by taking into account the correlations between the p_T and y distributions. Assuming that the uncertainty related to the correlation does not depend on the collision system and energy, this uncertainty was estimated using a large pp sample [45], by comparing the $A\varepsilon$ values obtained from p_T (y) dependent input shapes extracted in narrower y (p_T) intervals with those obtained using the corresponding shapes from the full y and p_T range. The remaining uncertainties on the $A\varepsilon$ were determined following the procedure described in detail in Ref. [14].

The normalization to MB events, N_{MB}^i , is computed as the product of the number of dimuon-triggered events and the inverse of the probability of having a dimuon trigger in a MB event, for the relevant centrality class i . This probability can be obtained with two methods, as explained in Ref. [47]; the difference is taken as the systematic uncertainty.

The average nuclear overlap function $\langle T_{AA} \rangle$ and number of participants $\langle N_{part} \rangle$ (i.e. the number of nucleons in the nuclei undergoing inelastic scattering) are obtained from a Glauber model fit of the V0 amplitude [49,50]. The uncertainty on the value of the V0 signal amplitude corresponding to the most central 90% of the total hadronic Pb–Pb cross section is $\pm 1\%$. This uncertainty is propagated into the definition of the centrality intervals as explained in Ref. [47].

The systematic uncertainties on the R_{AA} measurement as a function of centrality are summarized in Table 1.

Fig. 1 shows the R_{AA} as a function of the number of participants $\langle N_{part} \rangle$. The relationship between $\langle N_{part} \rangle$ and centrality is provided in Table 2. The J/ψ R_{AA} for $p_T < 0.3$ GeV/c (where coherent photoproduction would be highest) and $0.3 < p_T < 1.0$ GeV/c (where incoherent photoproduction could contribute) is compared with the R_{AA} for $1.0 < p_T < 2.0$ GeV/c (where hadroproduction dominates). The J/ψ R_{AA} in the p_T interval 0–0.3 GeV/c is significantly larger than the R_{AA} at larger transverse momenta, except for the most central events. It reaches a value of about 10 for the most peripheral events. This large increase is similar to the one of about a factor 7 measured at a lower center-of-mass energy [25]. The measurement in the interval 0.3–1 GeV/c is compatible with the one in 1–2 GeV/c except for the most peripheral events, where it is larger by roughly 2 standard deviations (σ). Further studies of the kinematic distribution of this signal could confirm the origin from incoherent photoproduction processes. Data are compared

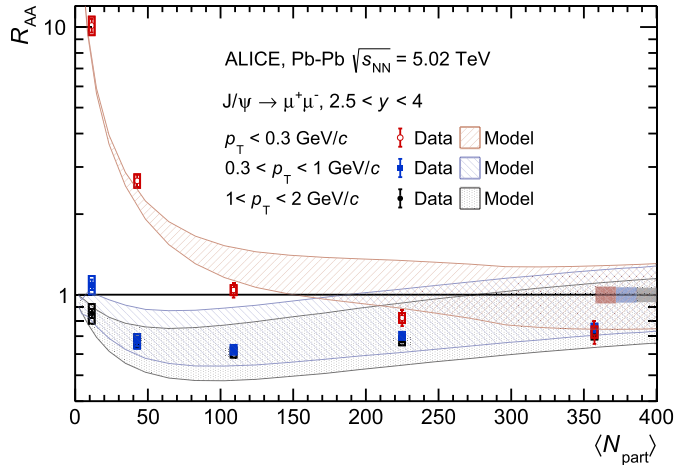


Fig. 1. J/ψ nuclear modification factor as a function of $\langle N_{part} \rangle$ measured in the rapidity range $2.5 < y < 4$ for three transverse momentum intervals. The vertical bars are the statistical uncertainties and the uncorrelated systematic uncertainties are represented as boxes. The centrality-correlated systematic uncertainties are shown as filled boxes at unity. Data are compared with predictions from Ref. [26], shown as bands.

with a model [26] that includes initial J/ψ production, J/ψ regeneration, and a J/ψ photoproduction component for $p_T < 0.3$ GeV/c. The uncertainty band of the theoretical predictions is mainly due to the variation of the shadowing factor. QGP effects on the photoproduced J/ψ are taken into account as well. The theoretical predictions well describe data in the p_T and centrality ranges considered.

The excess with respect to the expected hadronic production was quantified with the same procedure as used in Ref. [25]. For each centrality class, the hadronic J/ψ yield ($\frac{dN_{AA}^{i,h}}{dp_T}$) as a function of p_T is parameterized with:

$$\frac{dN_{AA}^{i,h}}{dp_T}(p_T) = \mathcal{N} \times \frac{d\sigma_{pp}^h}{dp_T}(p_T) \times R_{AA}^{i,h}(p_T) \times A\varepsilon^{i,h}(p_T). \quad (2)$$

The normalization factor \mathcal{N} is defined in such a way that the integral of the function in the p_T interval 1–8 GeV/c is equal to the measured number of J/ψ in the same interval, which is dominated by hadroproduction. The $\frac{d\sigma_{pp}^h}{dp_T}$ is taken from a fit to the pp cross section measured by ALICE at $\sqrt{s} = 5.02$ TeV [38] with either a power law function [51] or a Lévy-Tsallis function [52,53]. $R_{AA}^{i,h}$ is a fit to the measured nuclear modification factor as a function of p_T for the same centrality classes as presented above. For the central to semicentral intervals (0–50%) a Woods-Saxon like function [25] is used, with the parameter p_T^0 defining the 50% crossing point fixed to various values related to the J/ψ mass and average transverse momentum $\langle p_T \rangle$. This function was chosen since it can describe the transport model predictions for J/ψ production in heavy-ion collisions [54,55]. For the most peripheral intervals (50–90%), where the recombination effects in the QGP are expected to be smaller, a linear and a constant function are used. The fit is performed in two p_T intervals 0.65–15 GeV/c and 1–15 GeV/c, where the hadroproduction is the main contribution, and then extrapolated to $p_T = 0$. For the Woods-Saxon function, the quality of the low- p_T extrapolation is assessed by verifying that the functional form reproduces the measured R_{AA} in the most central events where the hadronic contribution is dominant. Finally, $A\varepsilon^{i,h}$ is a fit to the hadronic J/ψ acceptance and efficiency for the centrality class i , using a ratio of two Lévy-Tsallis functions. In order not to double-count the uncertainties on the pp cross section and on the Pb–Pb $A\varepsilon$, those were disregarded in the fit to the R_{AA} .

Table 2

Average number of participants, measured number of J/ψ , estimated number of hadronic J/ψ , difference between these two quantities and resulting J/ψ cross section for coherent photoproduction in the transverse momentum interval 0–0.3 GeV/c for the listed centrality classes. The first quoted uncertainty corresponds to the statistical uncertainty, the second to the centrality uncorrelated systematic uncertainty; in addition, a correlated systematic uncertainty of 6.6% applies to the cross section in all centrality classes. For the 0–10% centrality class, the quoted values correspond to a 95% confidence level interval.

Centrality class	$\langle N_{\text{part}} \rangle$	$N_{\text{raw}}^{J/\psi}$	$N_{\text{hadro}}^{J/\psi}$	$N_{\text{excess}}^{J/\psi}$	$d\sigma_{\text{coh}}^{J/\psi} / dy (\mu\text{b})$
0–10%	357.3 ± 0.8	$8351 \pm 762 \pm 312$	$8713 \pm 86 \pm 873$	< 2406 (95% CL)	< 230 (95% CL)
10–30%	225.0 ± 1.2	$9624 \pm 571 \pm 278$	$8274 \pm 60 \pm 742$	$1350 \pm 574 \pm 792$	$145 \pm 62 \pm 85$
30–50%	109.0 ± 1.1	$4280 \pm 225 \pm 105$	$2562 \pm 23 \pm 178$	$1718 \pm 226 \pm 207$	$179 \pm 24 \pm 22$
50–70%	42.7 ± 0.7	$2763 \pm 98 \pm 68$	$674 \pm 8 \pm 40$	$2089 \pm 98 \pm 79$	$216 \pm 10 \pm 12$
70–90%	11.3 ± 0.2	$1758 \pm 57 \pm 32$	$138 \pm 3 \pm 9$	$1620 \pm 57 \pm 33$	$167 \pm 6 \pm 12$

Each combination of different parametrizations and fit ranges results in a different hadronic J/ψ distribution as a function of p_T , which is then integrated in the p_T interval 0–0.3 GeV/c. The final numbers of expected hadronic J/ψ , defined as the averages of the obtained values, are listed in Table 2 (fourth column) together with the raw measured numbers of J/ψ (third column). For the expected hadronic yields, the statistical uncertainty comes from the statistical uncertainty on \mathcal{N} , which derives from the statistical uncertainty on the J/ψ raw yield in 1–8 GeV/c. The systematic uncertainty of the expected yields is taken as the quadratic sum of the standard deviation of the results obtained using different parametrizations and fit ranges, and the average of the individual systematic uncertainties for the variations (including contributions from all factors in Eq. (2)).

The estimated number of hadroproduced J/ψ is subtracted from the measured raw signal to obtain the number of J/ψ in excess (fifth column of Table 2). The measured number of J/ψ exceeds the hadronic production by 24σ in the 70–90% centrality class, 16σ in 50–70%, 5.6σ in 30–50% and 1.4σ in 10–30%. A 95% confidence interval when combining all uncertainties is provided in the centrality class 0–10% where no significant excess is observed within the current experimental uncertainties.

Assuming that the underlying process for the J/ψ excess is photoproduction, the number of coherently photoproduced J/ψ in $0 < p_T < 0.3$ GeV/c can be extracted after correcting the excess yield for the fractions of J/ψ from incoherent photoproduction (f_I) and from the decay of coherently photoproduced $\psi(2S)$ (f_D) as described in Ref. [7]. Those fractions were measured in UPC collisions at the same center-of-mass energy, although in a slightly different p_T interval, $p_T < 0.25$ GeV/c [7]. They were therefore recomputed for $p_T < 0.3$ GeV/c. The corresponding values and systematic uncertainties are $f_I = 0.089 \pm 0.034$ and $f_D = 0.066 \pm 0.013$. In the following it was assumed that these fractions are the same in UPC and hadronic collisions and that they do not depend significantly on the collision centrality. The first assumption seems realistic for f_D , although f_I might vary if the coherence is incomplete in the presence of hadronic interactions.

Finally, the cross section is obtained by correcting the excess yield for the branching ratio to OS dimuons, for the $A\epsilon$ factor estimated by means of STARlight [46] simulations embedded into data for each centrality class, taking into account that the coherently photoproduced J/ψ mesons are expected to be transversely polarized, and by normalizing to the integrated luminosity and the width of the rapidity range. The systematic uncertainties are summarized in Table 3. The uncertainties on the number of excess J/ψ are discussed above. The contributions from the $A\epsilon$ are the same as in Table 1, except for the one on the STARlight MC input, which is obtained as described in Ref. [7]. An additional systematic uncertainty of 2% due to the transverse momentum resolution was estimated by comparing the $A\epsilon$ obtained with or without the p_T selection at 0.3 GeV/c. The systematic uncertainty on the luminosity mainly originates from the uncertainty of the reference V0

Table 3

Systematic uncertainties on the coherent J/ψ cross section (notation is the same as in Table 1).

Source	Value (%)
Branching Ratio	0.5*
$N_{\text{excess}}^{J/\psi}$	2–58.7
f_I	2.9*
f_D	1.1*
Tracking eff.	0–0.5 + 3*
Trigger eff.	0–0.5 + 3.6*
Matching eff.	1*
MC input	0.1*
p_T selection	2*
Centrality limits	0.2–7
\mathcal{L}_{int}	2.5*

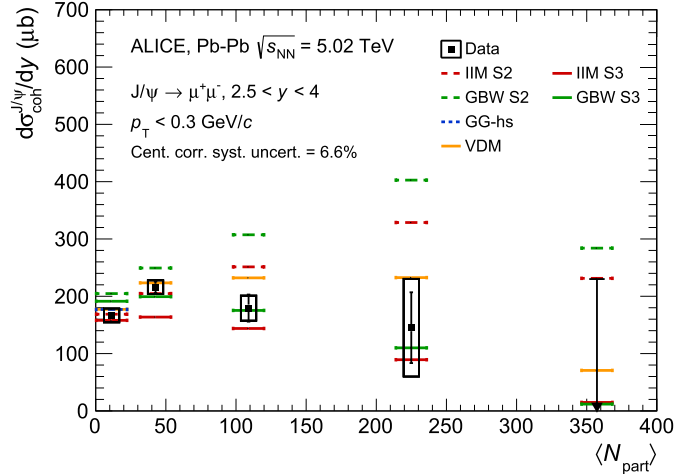


Fig. 2. J/ψ coherent photoproduction cross section as a function of $\langle N_{\text{part}} \rangle$ at forward rapidity in Pb–Pb collisions at $\sqrt{s_{\text{NN}}} = 5.02$ TeV. The vertical bars are the statistical uncertainties and the uncorrelated systematic uncertainties are represented as boxes. The centrality correlated systematic uncertainties are quoted in the legend. Results are compared with theoretical calculations from Ref. [33] (GG-hs), Ref. [32] (IIM S2 and S3, and GBW S2 and S3) and from Ref. [35] with updated Glauber calculations from Ref. [56] (VDM). The figure shows the integral of the cross section measurement as well as the corresponding theoretical model values in each centrality interval. Note that the most central bin, where only an upper limit is given, is half the size of the other intervals. Therefore, to evaluate the centrality dependence of J/ψ coherent photoproduction, both data and theory have to be multiplied by a factor of two.

trigger cross section measured with van der Meer scans [43]. The uncertainties on f_I and f_D are estimated as described in Ref. [7].

The coherent J/ψ photoproduction cross section at $\sqrt{s_{\text{NN}}} = 5.02$ TeV as a function of $\langle N_{\text{part}} \rangle$ is shown in Fig. 2. Empty boxes correspond to the uncorrelated systematic uncertainties. The correlated systematic uncertainty amounts to 6.6%, independent of centrality, and is quoted in the legend.

The result is compared with theoretical calculations that use an effective description based on UPC color dipole models. The GG-hs calculations [33] are based on models representing subnucleonic degrees of freedom as hot spots, whose number increases with increasing photon-target center of mass energy. The calculation is extended from protonic to nuclear targets using Glauber–Gribov formalism (GG) [33]. The photon flux is estimated in the same way as in the UPC case, but the integral is limited to the impact parameter range of the selected centrality class. The calculation from Ref. [56] is based on a vector dominance model, in which the photon fluctuates into a vector meson component that propagates through the nucleus and fragments into an on-shell vector meson. In this model, which will be referred to as VDM in the following, the photon flux is modified with respect to the one used in UPC calculations by considering only the photons that reach the geometrical region of the target nucleus outside of the overlap region. In the GBW calculation, the light cone color dipole formalism is used, while the IIM calculation is based on the Color Glass Condensate approach [32]. The GBW and IIM calculations provide two scenarios. In the first one (called S2 in Ref. [32]), the photon flux is modified in a similar way as for the VDM model. However, in contrast with the latter, an effective area is used in building the flux, which disregards the region of nuclear overlap. This prevents the flux and the resulting cross section from being progressively reduced towards more central collisions. In the second scenario (S3), an additional modification of the photon-nucleus cross section is introduced, in which the overlap region between the two nuclei is assumed not to contribute to coherent photoproduction resulting in significant reduction of the photoproduction cross sections towards more central collisions.

The hot-spot model prediction (GG-hs) is only available for the most peripheral centrality interval (70–90%) where the calculation is compatible with data. The other models provide predictions for all centrality intervals. The VDM model predicts a mild increase of the cross section in peripheral events, a flat evolution in semi-central events, and a decrease of the cross section in the most central events, in fair agreement with data. Notice that the figure shows the integral of the cross section in each centrality interval and the most central interval is half the size of the others. If one accounts for the interval width, the predictions for the most central interval would be twice as large, resulting in a rather mild decrease of the cross section with centrality. This model uses an optical Glauber model to describe the collision centrality, but a similar agreement with data can be obtained with a simplified relation between impact parameter and centrality [35]. The IIM and GBW models with unmodified photon-nucleus cross section (S2) predict a steady increase of the J/ψ coherent photoproduction cross section with centrality, once the width of the centrality intervals is properly accounted for. In data, this increasing trend is only observed for the two most peripheral intervals. In this scenario, the GBW model overestimates the data in all centrality intervals. The IIM model is in agreement with data in the first two centrality intervals, while it starts to deviate from the data by 2.1σ in the 30–50% centrality interval. The S3 version of the GBW and IIM models [32] excluding the nuclear overlap region from the photon-nucleus cross section calculation predicts a decrease of the cross section from semicentral to central events (similar to the one of Ref. [56], which, however, requires only a modification of the photon flux), and is compatible with the data in the full centrality range considering the current uncertainties. Since the transverse momentum of the coherently photoproduced vector meson is of the order of the inverse of the target size, the interaction occurring with the remaining nucleus fragment outside the overlap area would result in a larger average p_T and a wider p_T distribution for the photoproduced J/ψ . A measurement of the J/ψ p_T distribution at low p_T is therefore needed to clarify what is the underlying

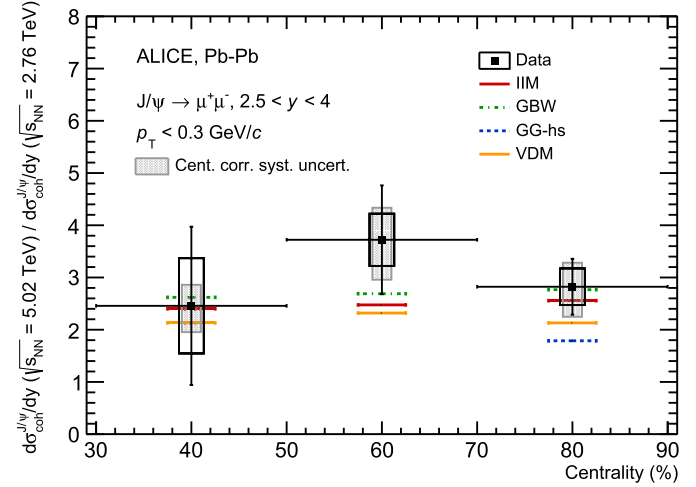


Fig. 3. J/ψ coherent photoproduction cross section ratio for two different energies ($\sqrt{s_{NN}} = 5.02$ TeV over $\sqrt{s_{NN}} = 2.76$ TeV) as a function of centrality. The data at $\sqrt{s_{NN}} = 2.76$ TeV are taken from Ref. [25]. The vertical lines are the statistical uncertainties while the open (filled) boxes are the centrality uncorrelated (correlated) systematic uncertainties. Results are compared with theoretical calculations from Ref. [33] (GG-hs), Ref. [32] (IIM and GBW) and from Ref. [35] with updated Glauber calculations from Ref. [56] (VDM).

mechanism leading to the observed distribution as a function of centrality.

The models described here provided predictions also for the measurement at $\sqrt{s_{NN}} = 2.76$ TeV [25]. The corresponding figure can be found in the Appendix A. The ratio of the measurements at $\sqrt{s_{NN}} = 5.02$ TeV and $\sqrt{s_{NN}} = 2.76$ TeV [25] is shown in Fig. 3. In the ratio, only the systematic uncertainty on the branching ratio cancels out. The centrality uncorrelated (correlated) systematic uncertainties in Table 3 are represented as open (filled) boxes in Fig. 3. The centrality correlated uncertainties are mainly due to the uncertainty on f_1 and f_D , which were asymmetric in the estimation performed at $\sqrt{s_{NN}} = 2.76$ TeV. The cross section increase with the center-of-mass energy does not depend significantly on the centrality. Fig. 3 shows that the hot-spot model tends to under-predict the increase of the cross section with the center-of-mass energy in peripheral hadronic interactions, while the other models are in fair agreement with the measured ratio in all centrality ranges within the large uncertainties. For the IIM and GBW models no distinction is done in this case between the scenarios with or without modification of the photon-nucleus cross section since their energy dependence is exactly the same.

In summary, this Letter reports the measurement of J/ψ production at very low p_T as a function of centrality in hadronic Pb–Pb collisions at $\sqrt{s_{NN}} = 5.02$ TeV at forward rapidity. The nuclear modification factor R_{AA} shows a large enhancement of the J/ψ yield for $p_T < 0.3$ GeV/c with respect to expectations from hadronic production. This excess, which was previously seen in more peripheral collisions, is now confirmed to be present for most of the total hadronic cross section, including in collisions with a large nuclear overlap, down to at least a level of 30% in centrality. The enhancement has a significance of 24σ in the 70–90% centrality class, 16σ in 50–70% and 5.6σ in the centrality class 30–50%. The reported observation extends previous measurements performed by the ALICE, LHCb and STAR Collaborations, supporting coherent photoproduction in hadronic collisions as the underlying mechanism. Based on this assumption, the corresponding cross section is extracted for the centrality classes 10–30%, 30–50%, 50–70% and 70–90% while an upper limit is given for 0–10%. The ratio of coherent photoproduction cross sections for $\sqrt{s_{NN}} = 5.02$ TeV over $\sqrt{s_{NN}} = 2.76$ TeV is extracted as a function of centrality and shows a flat dependence on centrality within uncertain-

ties. A set of theoretical calculations successfully used to describe coherent photoproduction in UPC, and modified to account for geometrical constraints on the photon flux in the selected centrality classes, is compared with the measurement. The cross section as a function of centrality is well described by two models, one implementing a modification of the photon flux only [56], and the other requiring an additional modification of the photon-nucleus cross section [32]. Additional measurements of the p_T -differential photoproduction cross section as a function of centrality and further comparison with models using different photoproduction scenarios would help to clarify the effect of the disruption of the nucleus and nucleons by hadronic interactions on the coherence condition of vector meson photoproduction.

Declaration of competing interest

The authors declare that they have no known competing financial interests or personal relationships that could have appeared to influence the work reported in this paper.

Data availability

Data will be made available on request.

Acknowledgements

The ALICE Collaboration would like to thank all its engineers and technicians for their invaluable contributions to the construction of the experiment and the CERN accelerator teams for the outstanding performance of the LHC complex. The ALICE Collaboration gratefully acknowledges the resources and support provided by all Grid centres and the Worldwide LHC Computing Grid (WLCG) collaboration. The ALICE Collaboration acknowledges the following funding agencies for their support in building and running the ALICE detector: A. I. Alikhanyan National Science Laboratory (Yerevan Physics Institute) Foundation (ANSL), State Committee of Science and World Federation of Scientists (WFS), Armenia; Austrian Academy of Sciences, Austrian Science Fund (FWF): [M 2467-N36] and Nationalstiftung für Forschung, Technologie und Entwicklung, Austria; Ministry of Communications and High Technologies, National Nuclear Research Center, Azerbaijan; Conselho Nacional de Desenvolvimento Científico e Tecnológico (CNPq), Fincionadora de Estudos e Projetos (Finep), Fundação de Amparo à Pesquisa do Estado de São Paulo (FAPESP) and Universidade Federal do Rio Grande do Sul (UFRGS), Brazil; Bulgarian Ministry of Education and Science, within the National Roadmap for Research Infrastructures 2020-2027 (object CERN), Bulgaria; Ministry of Education of China (MOEC), Ministry of Science & Technology of China (MSTC) and National Natural Science Foundation of China (NSFC), China; Ministry of Science and Education and Croatian Science Foundation, Croatia; Centro de Aplicaciones Tecnológicas y Desarrollo Nuclear (CEADEN), Cubaenergía, Cuba; Ministry of Education, Youth and Sports of the Czech Republic, Czech Republic; The Danish Council for Independent Research | Natural Sciences, the Villum Fonden and Danish National Research Foundation (DNRF), Denmark; Helsinki Institute of Physics (HIP), Finland; Commissariat à l'Énergie Atomique (CEA) and Institut National de Physique Nucléaire et de Physique des Particules (IN2P3) and Centre National de la Recherche Scientifique (CNRS), France; Bundesministerium für Bildung und Forschung (BMBF) and GSI Helmholtzzentrum für Schwerionenforschung GmbH, Germany; General Secretariat for Research and Technology, Ministry of Education, Research and Religious, Greece; National Research, Development and Innovation Office, Hungary; Department of Atomic Energy, Government of India (DAE), Department of Science and Technology, Government of India (DST), University Grants Commission, Government of India

(UGC) and Council of Scientific and Industrial Research (CSIR), India; National Research and Innovation Agency - BRIN, Indonesia; Istituto Nazionale di Fisica Nucleare (INFN), Italy; Japanese Ministry of Education, Culture, Sports, Science and Technology (MEXT) and Japan Society for the Promotion of Science (JSPS) KAKENHI, Japan; Consejo Nacional de Ciencia (CONACYT) y Tecnología, through Fondo de Cooperación Internacional en Ciencia y Tecnología (FONCICYT) and Dirección General de Asuntos del Personal Académico (DGAPA), Mexico; Nederlandse Organisatie voor Wetenschappelijk Onderzoek (NWO), Netherlands; The Research Council of Norway, Norway; Commission on Science and Technology for Sustainable Development in the South (COMSATS), Pakistan; Pontificia Universidad Católica del Perú, Peru; Ministry of Education and Science, National Science Centre and WUT ID-UB, Poland; Korea Institute of Science and Technology Information and National Research Foundation of Korea (NRF), Republic of Korea; Ministry of Education and Scientific Research, Institute of Atomic Physics, Ministry of Research and Innovation and Institute of Atomic Physics and University Politehnica of Bucharest, Romania; Ministry of Education, Science, Research and Sport of the Slovak Republic, Slovakia; National Research Foundation of South Africa, South Africa; Swedish Research Council (VR) and Knut and Alice Wallenberg Foundation (KAW), Sweden; European Organization for Nuclear Research, Switzerland; Suranaree University of Technology (SUT), National Science and Technology Development Agency (NSTDA) and National Science, Research and Innovation Fund (NSRF via PMU-B B05F650021), Thailand; Turkish Energy, Nuclear and Mineral Research Agency (TENMAK), Turkey; National Academy of Sciences of Ukraine, Ukraine; Science and Technology Facilities Council (STFC), United Kingdom; National Science Foundation of the United States of America (NSF) and United States Department of Energy, Office of Nuclear Physics (DOE NP), United States of America. In addition, individual groups or members have received support from: Marie Skłodowska Curie, Strong 2020 – Horizon 2020, European Research Council (grant nos. 824093, 896850, 950692), European Union; Academy of Finland (Center of Excellence in Quark Matter) (grant nos. 346327, 346328), Finland; Programa de Apoyos para la Superación del Personal Académico, UNAM, Mexico.

Appendix A. J/ψ photoproduction in Pb–Pb collisions at $\sqrt{s_{NN}} = 2.76$ TeV

Fig. A.1 shows the coherent photoproduction measured at $\sqrt{s_{NN}} = 2.76$ TeV [25]. Empty boxes correspond to the uncorrected systematic uncertainties. The centrality correlated systematic uncertainty mainly comes from the uncertainties on f_1 and f_D , which are asymmetric.

The data are compared with predictions from the same set of models that were described in detail in the paper to which this appendix is associated. The hot-spot model prediction (GG-hs) [33] is only available for the most peripheral centrality interval (70–90%) and it is found to overestimate the data. The other predictions are available for all centrality intervals. The centrality dependence of the models is similar to the one shown at $\sqrt{s_{NN}} = 5.02$ TeV. The IIM and GBW predictions [32] steadily increase with centrality in the scenario with unmodified photon-nucleus cross section (S2), while the use of an effective cross section where the overlap region between the two nuclei is assumed not to contribute to coherent photoproduction (S3) results in a reduction of the cross section toward more central collisions. However, both scenarios are compatible with data in the current uncertainties. Finally, the VDM calculations are in agreement with data in the most central events while they tend to overestimate data in the 50–70% and 70–90% centrality bins.

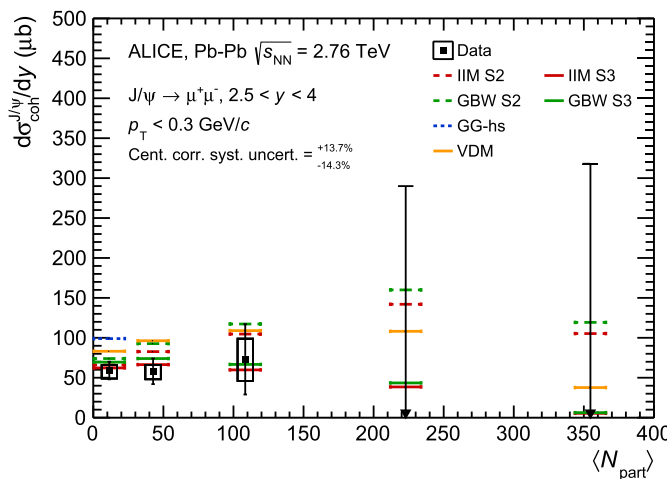


Fig. A.1. J/ψ coherent photoproduction cross section as a function of $\langle N_{\text{part}} \rangle$ at forward rapidity in Pb-Pb collisions at $\sqrt{s_{\text{NN}}} = 2.76 \text{ TeV}$ [25]. The vertical bars are the statistical uncertainties and the uncorrelated systematic uncertainties are represented as boxes. The centrality correlated systematic uncertainties are quoted in the legend. Results are compared with theoretical calculations from Ref. [33] (GG-hs), Ref. [32] (IIM S2 and S3, and GBW S2 and S3) and from Ref. [35] with updated Glauber calculations from Ref. [56] (VDM). The figure shows the integral of the cross section measurement as well as the corresponding theoretical model values in each centrality interval. Note that the most central bin, where only an upper limit is given, is half the size of the other intervals. Therefore, to evaluate the centrality dependence of J/ψ coherent photoproduction, both data and theory have to be multiplied by a factor of two.

References

- [1] K.J. Eskola, P. Paakkinen, H. Paukkunen, C.A. Salgado, EPPS16: nuclear parton distributions with LHC data, *Eur. Phys. J. C* **77** (3) (2017) 163, arXiv:1612.05741 [hep-ph].
- [2] V. Guzey, E. Kryshen, M. Strikman, M. Zhalov, Evidence for nuclear gluon shadowing from the ALICE measurements of PbPb ultraperipheral exclusive J/ψ production, *Phys. Lett. B* **726** (2013) 290–295, arXiv:1305.1724 [hep-ph].
- [3] V. Guzey, E. Kryshen, M. Strikman, M. Zhalov, Nuclear suppression from coherent J/ψ photoproduction at the Large Hadron Collider, *Phys. Lett. B* **816** (2021) 136202, arXiv:2008.10891 [hep-ph].
- [4] ALICE Collaboration, B. Abelev, et al., Coherent J/ψ photoproduction in ultra-peripheral Pb-Pb collisions at $\sqrt{s_{\text{NN}}} = 2.76 \text{ TeV}$, *Phys. Lett. B* **718** (2013) 1273–1283, arXiv:1209.3715 [nucl-ex].
- [5] ALICE Collaboration, E. Abbate, et al., Charmonium and e^+e^- pair photoproduction at mid-rapidity in ultra-peripheral Pb-Pb collisions at $\sqrt{s_{\text{NN}}} = 2.76 \text{ TeV}$, *Eur. Phys. J. C* **73** (11) (2013) 2617, arXiv:1305.1467 [nucl-ex].
- [6] CMS Collaboration, V. Khachatryan, et al., Coherent J/ψ photoproduction in ultra-peripheral PbPb collisions at $\sqrt{s_{\text{NN}}} = 2.76 \text{ TeV}$ with the CMS experiment, *Phys. Lett. B* **772** (2017) 489–511, arXiv:1605.06966 [nucl-ex].
- [7] ALICE Collaboration, S. Acharya, et al., Coherent J/ψ photoproduction at forward rapidity in ultra-peripheral Pb-Pb collisions at $\sqrt{s_{\text{NN}}} = 5.02 \text{ TeV}$, *Phys. Lett. B* **798** (2019) 134926, arXiv:1904.06272 [nucl-ex].
- [8] ALICE Collaboration, S. Acharya, et al., First measurement of the $|t|$ -dependence of coherent J/ψ photonuclear production, *Phys. Lett. B* **817** (2021) 136280, arXiv:2101.04623 [nucl-ex].
- [9] ALICE Collaboration, S. Acharya, et al., Coherent J/ψ and ψ' photoproduction at midrapidity in ultra-peripheral Pb-Pb collisions at $\sqrt{s_{\text{NN}}} = 5.02 \text{ TeV}$, *Eur. Phys. J. C* **81** (8) (2021) 712, arXiv:2101.04577 [nucl-ex].
- [10] M.G. Ryskin, Diffractive J/ψ electroproduction in LLA QCD, *Z. Phys. C* **57** (1993) 89–92.
- [11] S.R. Klein, H. Mäntysaari, Imaging the nucleus with high-energy photons, *Nat. Rev. Phys.* **1** (11) (2019) 662–674, arXiv:1910.10858 [hep-ex].
- [12] A.J. Baltz, The physics of ultraperipheral collisions at the LHC, *Phys. Rep.* **458** (2008) 1–171, arXiv:0706.3356 [nucl-ex].
- [13] ALICE Collaboration, B. Abelev, et al., Centrality, rapidity and transverse momentum dependence of J/ψ suppression in Pb-Pb collisions at $\sqrt{s_{\text{NN}}} = 2.76 \text{ TeV}$, *Phys. Lett. B* **734** (2014) 314–327, arXiv:1311.0214 [nucl-ex].
- [14] ALICE Collaboration, J. Adam, et al., Differential studies of inclusive J/ψ and $\psi(2S)$ production at forward rapidity in Pb-Pb collisions at $\sqrt{s_{\text{NN}}} = 2.76 \text{ TeV}$, *J. High Energy Phys.* **05** (2016) 179, arXiv:1506.08804 [nucl-ex].
- [15] ALICE Collaboration, S. Acharya, et al., Studies of J/ψ production at forward rapidity in Pb-Pb collisions at $\sqrt{s_{\text{NN}}} = 5.02 \text{ TeV}$, *J. High Energy Phys.* **02** (2020) 041, arXiv:1909.03158 [nucl-ex].
- [16] ALICE Collaboration, S. Acharya, et al., Centrality and transverse momentum dependence of inclusive J/ψ production at midrapidity in Pb-Pb collisions at $\sqrt{s_{\text{NN}}} = 5.02 \text{ TeV}$, *Phys. Lett. B* **805** (2020) 135434, arXiv:1910.14404 [nucl-ex].
- [17] T. Matsui, H. Satz, J/ψ suppression by quark-gluon plasma formation, *Phys. Lett. B* **178** (1986) 416–422.
- [18] P. Braun-Munzinger, J. Stachel, (Non)thermal aspects of charmonium production and a new look at J/ψ suppression, *Phys. Lett. B* **490** (2000) 196–202, arXiv:nucl-th/0007059 [nucl-th].
- [19] R.L. Thews, M. Schroedter, J. Rafelski, Enhanced J/ψ production in deconfined quark matter, *Phys. Rev. C* **63** (2001) 054905, arXiv:hep-ph/0007323 [hep-ph].
- [20] A. Andronic, P. Braun-Munzinger, K. Redlich, J. Stachel, Evidence for charmonium generation at the phase boundary in ultra-relativistic nuclear collisions, *Phys. Lett. B* **652** (2007) 259–261, arXiv:nucl-th/0701079.
- [21] ALICE Collaboration, S. Acharya, et al., Inclusive J/ψ production at forward and backward rapidity in p-Pb collisions at $\sqrt{s_{\text{NN}}} = 8.16 \text{ TeV}$, *J. High Energy Phys.* **07** (2018) 160, arXiv:1805.04381 [nucl-ex].
- [22] ALICE Collaboration, S. Acharya, et al., Prompt and non-prompt J/ψ production and nuclear modification at mid-rapidity in p-Pb collisions at $\sqrt{s_{\text{NN}}} = 5.02 \text{ TeV}$, *Eur. Phys. J. C* **78** (6) (2018) 466, arXiv:1802.00765 [nucl-ex].
- [23] CMS Collaboration, A.M. Sirunyan, et al., Measurement of prompt and non-prompt J/ψ production in pp and pPb collisions at $\sqrt{s_{\text{NN}}} = 5.02 \text{ TeV}$, *Eur. Phys. J. C* **77** (4) (2017) 269, arXiv:1702.01462 [nucl-ex].
- [24] LHCb Collaboration, R. Aaij, et al., Prompt and nonprompt J/ψ production and nuclear modification in pPb collisions at $\sqrt{s_{\text{NN}}} = 8.16 \text{ TeV}$, *Phys. Lett. B* **774** (2017) 159–178, arXiv:1706.07122 [hep-ex].
- [25] ALICE Collaboration, J. Adam, et al., Measurement of an excess in the yield of J/ψ at very low p_T in Pb-Pb collisions at $\sqrt{s_{\text{NN}}} = 2.76 \text{ TeV}$, *Phys. Rev. Lett.* **116** (22) (2016) 222301, arXiv:1509.08802 [nucl-ex].
- [26] W. Shi, W. Zha, B. Chen, Charmonium coherent photoproduction and hadroproduction with effects of quark gluon plasma, *Phys. Lett. B* **777** (2018) 399–405, arXiv:1710.00332 [nucl-th].
- [27] STAR Collaboration, J. Adam, et al., Observation of excess J/ψ yield at very low transverse momenta in Au+Au collisions at $\sqrt{s_{\text{NN}}} = 200 \text{ GeV}$ and U+U collisions at $\sqrt{s_{\text{NN}}} = 193 \text{ GeV}$, *Phys. Rev. Lett.* **123** (13) (2019) 132302, arXiv:1904.11658 [hep-ex].
- [28] LHCb Collaboration, R. Aaij, et al., J/ψ photoproduction in Pb-Pb peripheral collisions at $\sqrt{s_{\text{NN}}} = 5 \text{ TeV}$, *Phys. Rev. C* **105** (3) (2022) L032201, arXiv:2108.02681 [hep-ex].
- [29] ATLAS Collaboration, M. Aaboud, et al., Observation of centrality-dependent acoplanarity for muon pairs produced via two-photon scattering in Pb+Pb collisions at $\sqrt{s_{\text{NN}}} = 5.02 \text{ TeV}$ with the ATLAS detector, *Phys. Rev. Lett.* **121** (21) (2018) 212301, arXiv:1806.08708 [nucl-ex].
- [30] STAR Collaboration, J. Adam, et al., Low- p_T e^+e^- pair production in Au+Au collisions at $\sqrt{s_{\text{NN}}} = 200 \text{ GeV}$ and U+U collisions at $\sqrt{s_{\text{NN}}} = 193 \text{ GeV}$ at STAR, *Phys. Rev. Lett.* **121** (13) (2018) 132301, arXiv:1806.02295 [hep-ex].
- [31] ALICE Collaboration, S. Acharya, et al., Dielectron production at midrapidity at low transverse momentum in peripheral and semi-peripheral Pb-Pb collisions at $\sqrt{s_{\text{NN}}} = 5.02 \text{ TeV}$, *J. High Energy Phys.* **06** (2023) 024, arXiv:2204.11732 [nucl-ex].
- [32] M. Gay Ducati, S. Martins, Heavy meson photoproduction in peripheral AA collisions, *Phys. Rev. D* **97** (11) (2018) 116013, arXiv:1804.09836 [hep-ph].
- [33] J. Cepila, J.G. Contreras, M. Krelin, Coherent and incoherent J/ψ photonuclear production in an energy-dependent hot-spot model, *Phys. Rev. C* **97** (2) (2018) 024901, arXiv:1711.01855 [hep-ph].
- [34] W. Zha, S.R. Klein, R. Ma, L. Ruan, T. Todoroki, Z. Tang, Z. Xu, C. Yang, Q. Yang, S. Yang, Coherent J/ψ photoproduction in hadronic heavy-ion collisions, *Phys. Rev. C* **97** (4) (2018) 044910, arXiv:1705.01460 [nucl-th].
- [35] M. Klusek-Gawenda, A. Szczurek, Photoproduction of J/ψ mesons in peripheral and semicentral heavy ion collisions, *Phys. Rev. C* **93** (4) (2016) 044912, arXiv:1509.03173 [nucl-th].
- [36] L. Jenkovszky, V. Libov, M.V.T. Machado, Regge phenomenology and coherent photoproduction of J/ψ in peripheral heavy ion collisions, *Phys. Lett. B* **827** (2022) 137004, arXiv:2202.02162 [hep-ph].
- [37] J.G. Contreras, Gluon shadowing at small x from coherent J/ψ photoproduction data at energies available at the CERN Large Hadron Collider, *Phys. Rev. C* **96** (1) (2017) 015203, arXiv:1610.03350 [nucl-ex].
- [38] ALICE Collaboration, S. Acharya, et al., Inclusive quarkonium production in pp collisions at $\sqrt{s} = 5.02 \text{ TeV}$, *Eur. Phys. J. C* **83** (1) (2023) 61, arXiv:2109.15240 [nucl-ex].
- [39] ALICE Collaboration, K. Aamodt, et al., The ALICE experiment at the CERN LHC, *J. Instrum.* **3** (2008) S08002.
- [40] ALICE Collaboration, B. Abelev, et al., Performance of the ALICE experiment at the CERN LHC, *Int. J. Mod. Phys. A* **29** (2014) 1430044, arXiv:1402.4476 [nucl-ex].
- [41] ALICE Collaboration, B. Abelev, et al., Centrality determination of Pb-Pb collisions at $\sqrt{s_{\text{NN}}} = 2.76 \text{ TeV}$ with ALICE, *Phys. Rev. C* **88** (4) (2013) 044909, arXiv:1301.4361 [nucl-ex].
- [42] ALICE Collaboration, B. Abelev, et al., Measurement of the cross section for electromagnetic dissociation with neutron emission in Pb-Pb collisions at $\sqrt{s_{\text{NN}}} = 2.76 \text{ TeV}$, *Phys. Rev. Lett.* **109** (2012) 252302, arXiv:1203.2436 [nucl-ex].

- [43] ALICE Collaboration, S. Acharya, et al., ALICE luminosity determination for Pb–Pb collisions at $\sqrt{s_{NN}} = 5.02$ TeV, arXiv:2204.10148 [nucl-ex].
- [44] ALICE Collaboration, J. Adam, et al., Quarkonium signal extraction in ALICE, ALICE-PUBLIC-2015-006, <https://cds.cern.ch/record/2060096>.
- [45] ALICE Collaboration, S. Acharya, et al., Energy dependence of forward-rapidity J/ψ and $\psi(2S)$ production in pp collisions at the LHC, Eur. Phys. J. C 77 (6) (2017) 392, arXiv:1702.00557 [hep-ex].
- [46] S.R. Klein, J. Nystrand, J. Seger, Y. Gorbunov, J. Butterworth, STARlight: a Monte Carlo simulation program for ultra-peripheral collisions of relativistic ions, Comput. Phys. Commun. 212 (2017) 258–268, arXiv:1607.03838 [hep-ph].
- [47] ALICE Collaboration, J. Adam, et al., J/ψ suppression at forward rapidity in Pb–Pb collisions at $\sqrt{s_{NN}} = 5.02$ TeV, Phys. Lett. B 766 (2017) 212–224, arXiv:1606.08197 [nucl-ex].
- [48] Particle Data Group Collaboration, P.A. Zyla, et al., Review of particle physics, PTEP 2020 (8) (2020) 083C01.
- [49] ALICE Collaboration, J. Adam, et al., Centrality dependence of the charged-particle multiplicity density at midrapidity in Pb–Pb collisions at $\sqrt{s_{NN}} = 5.02$ TeV, Phys. Rev. Lett. 116 (22) (2016) 222302, arXiv:1512.06104 [nucl-ex].
- [50] D. d'Enterria, C. Loizides, Progress in the Glauber model at collider energies, Annu. Rev. Nucl. Part. Sci. 71 (2021) 315–344, arXiv:2011.14909 [hep-ph].
- [51] F. Bossù, Z.C. del Valle, A. de Falco, M. Gagliardi, S. Grigoryan, G. Martinez Garcia, Phenomenological interpolation of the inclusive J/ψ cross section to proton-proton collisions at 2.76 TeV and 5.5 TeV, arXiv:1103.2394 [nucl-ex].
- [52] C. Tsallis, Possible generalization of Boltzmann-Gibbs statistics, J. Stat. Phys. 52 (1988) 479–487.
- [53] STAR Collaboration, B.I. Abelev, et al., Strange particle production in p+p collisions at $s^{**}(1/2) = 200$ -GeV, Phys. Rev. C 75 (2007) 064901, arXiv:nucl-ex/0607033.
- [54] X. Zhao, R. Rapp, Medium modifications and production of charmonia at LHC, Nucl. Phys. A 859 (2011) 114–125, arXiv:1102.2194 [hep-ph].
- [55] Y.-p. Liu, Z. Qu, N. Xu, P.-f. Zhuang, J/ψ transverse momentum distribution in high energy nuclear collisions at RHIC, Phys. Lett. B 678 (2009) 72–76, arXiv: 0901.2757 [nucl-th].
- [56] M. Klusek-Gawenda, R. Rapp, W. Schäfer, A. Szczurek, Dilepton radiation in heavy-ion collisions at small transverse momentum, Phys. Lett. B 790 (2019) 339–344, arXiv:1809.07049 [nucl-th].

ALICE Collaboration

- S. Acharya 123, 131, , D. Adamová 85, , A. Adler 69, G. Aglieri Rinella 32, , M. Agnello 29, , N. Agrawal 50, , Z. Ahammed 131, , S. Ahmad 15, , S.U. Ahn 70, , I. Ahuja 37, , A. Akindinov 139, , M. Al-Turany 97, , D. Aleksandrov 139, , B. Alessandro 55, , H.M. Alfanda 6, , R. Alfaro Molina 66, , B. Ali 15, , Y. Ali 13, A. Alici 25, , N. Alizadehvandchali 112, , A. Alkin 32, , J. Alme 20, , G. Alococo 51, , T. Alt 63, , I. Altsybeev 139, , M.N. Anaam 6, , C. Andrei 45, , A. Andronic 134, , V. Anguelov 94, , F. Antinori 53, , P. Antonioli 50, , C. Anuj 15, , N. Apadula 73, , L. Aphecetche 102, , H. Appelshäuser 63, , S. Arcelli 25, , R. Arnaldi 55, , I.C. Arsene 19, , M. Arslanbekov 136, , A. Augustinus 32, , R. Averbeck 97, , S. Aziz 127, , M.D. Azmi 15, , A. Badalà 52, , Y.W. Baek 40, , X. Bai 97, , R. Bailhache 63, , Y. Bailung 47, , R. Bala 90, , A. Balbino 29, , A. Baldissari 126, , B. Balis 2, , D. Banerjee 4, , Z. Banoo 90, , R. Barbera 26, , L. Barioglio 95, , M. Barlou 77, G.G. Barnaföldi 135, , L.S. Barnby 84, , V. Barret 123, , L. Barreto 108, , C. Bartels 115, , K. Barth 32, , E. Bartsch 63, , F. Baruffaldi 27, , N. Bastid 123, , S. Basu 74, , G. Batigne 102, , D. Battistini 95, , B. Batyunya 140, , D. Bauri 46, J.L. Bazo Alba 100, , I.G. Bearden 82, , C. Beattie 136, , P. Becht 97, , D. Behera 47, , I. Belikov 125, , A.D.C. Bell Hechavarria 134, , F. Bellini 25, , R. Bellwied 112, , S. Belokurova 139, , V. Belyaev 139, , G. Bencedi 135, 64, , S. Beole 24, , A. Bercuci 45, , Y. Berdnikov 139, , A. Berdnikova 94, , L. Bergmann 94, , M.G. Besoiu 62, , L. Betev 32, , P.P. Bhaduri 131, , A. Bhasin 90, , I.R. Bhat 90, M.A. Bhat 4, , B. Bhattacharjee 41, , L. Bianchi 24, , N. Bianchi 48, , J. Bielčík 35, , J. Bielčíková 85, , J. Biernat 105, , A. Bilandžić 95, , G. Biro 135, , S. Biswas 4, , J.T. Blair 106, , D. Blau 139, , M.B. Blidaru 97, , N. Bluhm 38, C. Blume 63, , G. Boca 21, 54, , F. Bock 86, , T. Bodova 20, , A. Bogdanov 139, , S. Boi 22, , J. Bok 57, , L. Boldizsár 135, , A. Bolozdynya 139, , M. Bombara 37, , P.M. Bond 32, , G. Bonomi 130, 54, , H. Borel 126, , A. Borissov 139, , H. Bossi 136, , E. Botta 24, , L. Bratrud 63, , P. Braun-Munzinger 97, , M. Bregant 108, , M. Broz 35, , G.E. Bruno 96, 31, , M.D. Buckland 115, , D. Budnikov 139, , H. Buesching 63, , S. Bufalino 29, , O. Bugnon 102, , P. Buhler 101, , Z. Buthelezi 67, 119, , J.B. Butt 13, A. Bylinkin 114, , S.A. Bysiak 105, M. Cai 27, 6, , H. Caines 136, , A. Caliva 97, , E. Calvo Villar 100, , J.M.M. Camacho 107, , P. Camerini 23, , F.D.M. Canedo 108, , M. Carabas 122, , F. Carnesecchi 32, , R. Caron 124, 126, , J. Castillo Castellanos 126, , F. Catalano 29, , C. Ceballos Sanchez 140, , I. Chakaberia 73, , P. Chakraborty 46, , S. Chandra 131, , S. Chapelard 32, , M. Chartier 115, , S. Chattopadhyay 131, , S. Chattopadhyay 98, , T.G. Chavez 44, , T. Cheng 6, , C. Cheshkov 124, , B. Cheynis 124, , V. Chibante Barroso 32, , D.D. Chinellato 109, , E.S. Chizzali 95, , J. Cho 57, , S. Cho 57, , P. Chochula 32, , P. Christakoglou 83, ,

- C.H. Christensen 82, ID, P. Christiansen 74, ID, T. Chujo 121, ID, M. Ciacco 29, ID, C. Cicalo 51, ID, L. Cifarelli 25, ID, F. Cindolo 50, ID, M.R. Ciupek 97, G. Clai 50, III, F. Colamaria 49, ID, J.S. Colburn 99, D. Colella 96, 31, ID, A. Collu 73, M. Colocci 32, ID, M. Concias 55, ID, IV, G. Conesa Balbastre 72, ID, Z. Conesa del Valle 127, ID, G. Contin 23, ID, J.G. Contreras 35, ID, M.L. Coquet 126, ID, T.M. Cormier 86, I, P. Cortese 129, 55, ID, M.R. Cosentino 110, ID, F. Costa 32, ID, S. Costanza 21, 54, ID, P. Crochet 123, ID, R. Cruz-Torres 73, ID, E. Cuautle 64, P. Cui 6, ID, L. Cunqueiro 86, A. Dainese 53, ID, M.C. Danisch 94, ID, A. Danu 62, ID, P. Das 79, ID, P. Das 4, ID, S. Das 4, ID, S. Dash 46, ID, R.M.H. David 44, A. De Caro 28, ID, G. de Cataldo 49, ID, L. De Cilladi 24, ID, J. de Cuveland 38, A. De Falco 22, ID, D. De Gruttola 28, ID, N. De Marco 55, ID, C. De Martin 23, ID, S. De Pasquale 28, ID, S. Deb 47, ID, H.F. Degenhardt 108, K.R. Deja 132, R. Del Grande 95, ID, L. Dello Stritto 28, ID, W. Deng 6, ID, P. Dhankher 18, ID, D. Di Bari 31, ID, A. Di Mauro 32, ID, R.A. Diaz 140, 7, ID, T. Dietel 111, ID, Y. Ding 124, 6, ID, R. Divià 32, ID, D.U. Dixit 18, ID, Ø. Djupsland 20, U. Dmitrieva 139, ID, A. Dobrin 62, ID, B. Dönigus 63, ID, A.K. Dubey 131, ID, J.M. Dubinski 132, ID, A. Dubla 97, ID, S. Dudi 89, ID, P. Dupieux 123, ID, M. Durkac 104, N. Dzalaiova 12, T.M. Eder 134, ID, R.J. Ehlers 86, ID, V.N. Eikeland 20, F. Eisenhut 63, ID, D. Elia 49, ID, B. Erazmus 102, ID, F. Ercolelli 25, ID, F. Erhardt 88, ID, M.R. Ersdal 20, B. Espagnon 127, ID, G. Eulisse 32, ID, D. Evans 99, ID, S. Evdokimov 139, ID, L. Fabbietti 95, ID, M. Faggin 27, ID, J. Faivre 72, ID, F. Fan 6, ID, W. Fan 73, ID, A. Fantoni 48, ID, M. Fasel 86, ID, P. Fecchio 29, A. Feliciello 55, ID, G. Feofilov 139, ID, A. Fernández Téllez 44, ID, M.B. Ferrer 32, ID, A. Ferrero 126, ID, A. Ferretti 24, ID, V.J.G. Feuillard 94, ID, J. Figiel 105, ID, V. Filova 35, ID, D. Finogeev 139, ID, F.M. Fionda 51, ID, G. Fiorenza 96, F. Flor 112, ID, A.N. Flores 106, ID, S. Foertsch 67, ID, I. Fokin 94, ID, S. Fokin 139, ID, E. Fragiacomo 56, ID, E. Frajna 135, ID, U. Fuchs 32, ID, N. Funicello 28, ID, C. Furget 72, ID, A. Furs 139, ID, J.J. Gaardhøje 82, ID, M. Gagliardi 24, ID, A.M. Gago 100, ID, A. Gal 125, C.D. Galvan 107, ID, P. Ganoti 77, ID, C. Garabatos 97, ID, J.R.A. Garcia 44, ID, E. Garcia-Solis 9, ID, K. Garg 102, ID, C. Gargiulo 32, ID, A. Garibbi 80, K. Garner 134, E.F. Gauger 106, ID, A. Gautam 114, ID, M.B. Gay Ducati 65, ID, M. Germain 102, ID, S.K. Ghosh 4, M. Giacalone 25, ID, P. Gianotti 48, ID, P. Giubellino 97, 55, ID, P. Giubilato 27, ID, A.M.C. Glaenzer 126, ID, P. Glässel 94, ID, E. Glimos 118, ID, D.J.Q. Goh 75, V. Gonzalez 133, ID, L.H. González-Trueba 66, ID, S. Gorbunov 38, M. Gorgon 2, ID, L. Görlich 105, ID, S. Gotovac 33, V. Grabski 66, ID, L.K. Graczykowski 132, ID, E. Grecka 85, ID, L. Greiner 73, ID, A. Grelli 58, ID, C. Grigoras 32, ID, V. Grigoriev 139, ID, S. Grigoryan 140, 1, ID, F. Grossa 32, ID, J.F. Grosse-Oetringhaus 32, ID, R. Grossi 97, ID, D. Grund 35, ID, G.G. Guardiano 109, ID, R. Guernane 72, ID, M. Guilbaud 102, ID, K. Gulbrandsen 82, ID, T. Gunji 120, ID, W. Guo 6, ID, A. Gupta 90, ID, R. Gupta 90, ID, S.P. Guzman 44, ID, L. Gyulai 135, ID, M.K. Habib 97, C. Hadjidakis 127, ID, H. Hamagaki 75, ID, M. Hamid 6, Y. Han 137, ID, R. Hannigan 106, ID, M.R. Haque 132, ID, A. Harlenderova 97, J.W. Harris 136, ID, A. Harton 9, ID, J.A. Hasenbichler 32, H. Hassan 86, ID, D. Hatzifotiadou 50, ID, P. Hauer 42, ID, L.B. Havener 136, ID, S.T. Heckel 95, ID, E. Hellbär 97, ID, H. Helstrup 34, ID, T. Herman 35, ID, G. Herrera Corral 8, ID, F. Herrmann 134, K.F. Hetland 34, ID, B. Heybeck 63, ID, H. Hillemanns 32, ID, C. Hills 115, ID, B. Hippolyte 125, ID, B. Hofman 58, ID, B. Hohlweger 83, ID, J. Honermann 134, ID, G.H. Hong 137, ID, D. Horak 35, ID, A. Horzyk 2, ID, R. Hosokawa 14, Y. Hou 6, ID, P. Hristov 32, ID, C. Hughes 118, ID, P. Huhn 63, L.M. Huhta 113, ID, C.V. Hulse 127, ID, T.J. Humanic 87, ID, H. Hushnud 98, A. Hutson 112, ID, D. Hutter 38, ID, J.P. Iddon 115, ID, R. Ilkaev 139, H. Ilyas 13, ID, M. Inaba 121, ID, G.M. Innocenti 32, ID, M. Ippolitov 139, ID, A. Isakov 85, ID, T. Isidori 114, ID, M.S. Islam 98, ID, M. Ivanov 97, ID, V. Ivanov 139, ID, V. Izucheev 139, M. Jablonski 2, ID, B. Jacak 73, ID, N. Jacazio 32, ID, P.M. Jacobs 73, ID, S. Jadlovska 104, J. Jadlovsky 104, L. Jaffe 38, C. Jahnke 109, ID, M.A. Janik 132, ID, T. Janson 69, M. Jercic 88, O. Jevons 99, A.A.P. Jimenez 64, ID, F. Jonas 86, ID, P.G. Jones 99, J.M. Jowett 32, 97, ID, J. Jung 63, ID, M. Jung 63, ID, A. Junque 32, ID, A. Jusko 99, ID, M.J. Kabus 32, 132, ID,

- J. Kaewjai ¹⁰³, P. Kalinak ^{59, ID}, A.S. Kalteyer ^{97, ID}, A. Kalweit ^{32, ID}, V. Kaplin ^{139, ID}, A. Karasu Uysal ^{71, ID}, D. Karatovic ^{88, ID}, O. Karavichev ^{139, ID}, T. Karavicheva ^{139, ID}, P. Karczmarczyk ^{132, ID}, E. Karpechev ^{139, ID}, V. Kashyap ⁷⁹, A. Kazantsev ¹³⁹, U. Kebschull ^{69, ID}, R. Keidel ^{138, ID}, D.L.D. Keijdener ⁵⁸, M. Keil ^{32, ID}, B. Ketzer ^{42, ID}, A.M. Khan ^{6, ID}, S. Khan ^{15, ID}, A. Khanzadeev ^{139, ID}, Y. Kharlov ^{139, ID}, A. Khatun ^{15, ID}, A. Khuntia ^{105, ID}, B. Kileng ^{34, ID}, B. Kim ^{16, ID}, C. Kim ^{16, ID}, D.J. Kim ^{113, ID}, E.J. Kim ^{68, ID}, J. Kim ^{137, ID}, J.S. Kim ^{40, ID}, J. Kim ^{94, ID}, J. Kim ^{68, ID}, M. Kim ^{94, ID}, S. Kim ^{17, ID}, T. Kim ^{137, ID}, S. Kirsch ^{63, ID}, I. Kisel ^{38, ID}, S. Kiselev ^{139, ID}, A. Kisiel ^{132, ID}, J.P. Kitowski ^{2, ID}, J.L. Klay ^{5, ID}, J. Klein ^{32, ID}, S. Klein ^{73, ID}, C. Klein-Bösing ^{134, ID}, M. Kleiner ^{63, ID}, T. Klemenz ^{95, ID}, A. Kluge ^{32, ID}, A.G. Knospe ^{112, ID}, C. Kobdaj ^{103, ID}, T. Kollegger ⁹⁷, A. Kondratyev ^{140, ID}, N. Kondratyeva ^{139, ID}, E. Kondratyuk ^{139, ID}, J. Konig ^{63, ID}, S.A. Konigstorfer ^{95, ID}, P.J. Konopka ^{32, ID}, G. Kornakov ^{132, ID}, S.D. Koryciak ^{2, ID}, A. Kotliarov ^{85, ID}, O. Kovalenko ^{78, ID}, V. Kovalenko ^{139, ID}, M. Kowalski ^{105, ID}, I. Králik ^{59, ID}, A. Kravčáková ^{37, ID}, L. Kreis ⁹⁷, M. Krivda ^{99,59, ID}, F. Krizek ^{85, ID}, K. Krizkova Gajdosova ^{35, ID}, M. Kroesen ^{94, ID}, M. Krüger ^{63, ID}, D.M. Krupova ^{35, ID}, E. Kryshen ^{139, ID}, M. Krzewicki ³⁸, V. Kučera ^{32, ID}, C. Kuhn ^{125, ID}, P.G. Kuijer ^{83, ID}, T. Kumaoka ¹²¹, D. Kumar ¹³¹, L. Kumar ^{89, ID}, N. Kumar ⁸⁹, S. Kundu ^{32, ID}, P. Kurashvili ^{78, ID}, A. Kurepin ^{139, ID}, A.B. Kurepin ^{139, ID}, S. Kushpil ^{85, ID}, J. Kvapil ^{99, ID}, M.J. Kweon ^{57, ID}, J.Y. Kwon ^{57, ID}, Y. Kwon ^{137, ID}, S.L. La Pointe ^{38, ID}, P. La Rocca ^{26, ID}, Y.S. Lai ⁷³, A. Lakrathok ¹⁰³, M. Lamanna ^{32, ID}, R. Langoy ^{117, ID}, P. Larionov ^{48, ID}, E. Laudi ^{32, ID}, L. Lautner ^{32,95, ID}, R. Lavicka ^{101, ID}, T. Lazareva ^{139, ID}, R. Lea ^{130,54, ID}, J. Lehrbach ^{38, ID}, R.C. Lemmon ^{84, ID}, I. León Monzón ^{107, ID}, M.M. Lesch ^{95, ID}, E.D. Lesser ^{18, ID}, M. Lettrich ⁹⁵, P. Lévai ^{135, ID}, X. Li ¹⁰, X.L. Li ⁶, J. Lien ^{117, ID}, R. Lietava ^{99, ID}, B. Lim ^{16, ID}, S.H. Lim ^{16, ID}, V. Lindenstruth ^{38, ID}, A. Lindner ⁴⁵, C. Lippmann ^{97, ID}, A. Liu ^{18, ID}, D.H. Liu ^{6, ID}, J. Liu ^{115, ID}, I.M. Lofnes ^{20, ID}, V. Loginov ¹³⁹, C. Loizides ^{86, ID}, P. Loncar ^{33, ID}, J.A. Lopez ^{94, ID}, X. Lopez ^{123, ID}, E. López Torres ^{7, ID}, P. Lu ^{97,116, ID}, J.R. Luhder ^{134, ID}, M. Lunardon ^{27, ID}, G. Luparello ^{56, ID}, Y.G. Ma ^{39, ID}, A. Maevskaya ¹³⁹, M. Mager ^{32, ID}, T. Mahmoud ⁴², A. Maire ^{125, ID}, M. Malaev ^{139, ID}, N.M. Malik ^{90, ID}, Q.W. Malik ¹⁹, S.K. Malik ^{90, ID}, L. Malinina ^{140, ID, VII}, D. Mal'Kevich ^{139, ID}, D. Mallick ^{79, ID}, N. Mallick ^{47, ID}, G. Mandaglio ^{30,52, ID}, V. Manko ^{139, ID}, F. Manso ^{123, ID}, V. Manzari ^{49, ID}, Y. Mao ^{6, ID}, G.V. Margagliotti ^{23, ID}, A. Margotti ^{50, ID}, A. Marín ^{97, ID}, C. Markert ^{106, ID}, M. Marquard ⁶³, N.A. Martin ⁹⁴, P. Martinengo ^{32, ID}, J.L. Martinez ¹¹², M.I. Martínez ^{44, ID}, G. Martínez García ^{102, ID}, S. Masciocchi ^{97, ID}, M. Masera ^{24, ID}, A. Masoni ^{51, ID}, L. Massacrier ^{127, ID}, A. Mastroserio ^{128,49, ID}, A.M. Mathis ^{95, ID}, O. Matonoha ^{74, ID}, P.F.T. Matuoka ¹⁰⁸, A. Matyja ^{105, ID}, C. Mayer ^{105, ID}, A.L. Mazuecos ^{32, ID}, F. Mazzaschi ^{24, ID}, M. Mazzilli ^{32, ID}, J.E. Mdhuli ^{119, ID}, A.F. Mechler ⁶³, Y. Melikyan ^{139, ID}, A. Menchaca-Rocha ^{66, ID}, E. Meninno ^{101,28, ID}, A.S. Menon ^{112, ID}, M. Meres ^{12, ID}, S. Mhlanga ^{111,67}, Y. Miake ¹²¹, L. Micheletti ^{55, ID}, L.C. Migliorin ¹²⁴, D.L. Mihaylov ^{95, ID}, K. Mikhaylov ^{140,139, ID}, A.N. Mishra ^{135, ID}, D. Miśkowiec ^{97, ID}, A. Modak ^{4, ID}, A.P. Mohanty ^{58, ID}, B. Mohanty ⁷⁹, M. Mohisin Khan ^{15, ID, V}, M.A. Molander ^{43, ID}, Z. Moravcova ^{82, ID}, C. Mordasini ^{95, ID}, D.A. Moreira De Godoy ^{134, ID}, I. Morozov ^{139, ID}, A. Morsch ^{32, ID}, T. Mrnjavac ^{32, ID}, V. Muccifora ^{48, ID}, E. Mudnic ³³, S. Muhuri ^{131, ID}, J.D. Mulligan ^{73, ID}, A. Mulliri ²², M.G. Munhoz ^{108, ID}, R.H. Munzer ^{63, ID}, H. Murakami ^{120, ID}, S. Murray ^{111, ID}, L. Musa ^{32, ID}, J. Musinsky ^{59, ID}, J.W. Myrcha ^{132, ID}, B. Naik ^{119, ID}, R. Nair ^{78, ID}, B.K. Nandi ^{46, ID}, R. Nania ^{50, ID}, E. Nappi ^{49, ID}, A.F. Nassirpour ^{74, ID}, A. Nath ^{94, ID}, C. Nattrass ^{118, ID}, A. Neagu ¹⁹, A. Negru ¹²², L. Nellen ^{64, ID}, S.V. Nesbo ³⁴, G. Neskovic ^{38, ID}, D. Nesterov ^{139, ID}, B.S. Nielsen ^{82, ID}, E.G. Nielsen ^{82, ID}, S. Nikolaev ^{139, ID}, S. Nikulin ^{139, ID}, V. Nikulin ^{139, ID}, F. Noferini ^{50, ID}, S. Noh ^{11, ID}, P. Nomokonov ^{140, ID}, J. Norman ^{115, ID}, N. Novitzky ^{121, ID}, P. Nowakowski ^{132, ID}, A. Nyanin ^{139, ID}, J. Nystrand ^{20, ID}, M. Ogino ^{75, ID}, A. Ohlson ^{74, ID}, V.A. Okorokov ^{139, ID}, J. Oleniacz ^{132, ID}, A.C. Oliveira Da Silva ^{118, ID},

- M.H. Oliver ^{136, ID}, A. Onnerstad ^{113, ID}, C. Oppedisano ^{55, ID}, A. Ortiz Velasquez ^{64, ID}, A. Oskarsson ⁷⁴, J. Otwinowski ^{105, ID}, M. Oya ⁹², K. Oyama ^{75, ID}, Y. Pachmayer ^{94, ID}, S. Padhan ^{46, ID}, D. Pagano ^{130, 54, ID}, G. Paić ^{64, ID}, A. Palasciano ^{49, ID}, S. Panebianco ^{126, ID}, J. Park ^{57, ID}, J.E. Parkkila ^{32, 113, ID}, S.P. Pathak ¹¹², R.N. Patra ⁹⁰, B. Paul ^{22, ID}, H. Pei ^{6, ID}, T. Peitzmann ^{58, ID}, X. Peng ^{6, ID}, L.G. Pereira ^{65, ID}, H. Pereira Da Costa ^{126, ID}, D. Peresunko ^{139, ID}, G.M. Perez ^{7, ID}, S. Perrin ^{126, ID}, Y. Pestov ¹³⁹, V. Petráček ^{35, ID}, V. Petrov ^{139, ID}, M. Petrovici ^{45, ID}, R.P. Pezzi ^{102, 65, ID}, S. Piano ^{56, ID}, M. Pikna ^{12, ID}, P. Pillot ^{102, ID}, O. Pinazza ^{50, 32, ID}, L. Pinsky ¹¹², C. Pinto ^{95, 26, ID}, S. Pisano ^{48, ID}, M. Płoskoń ^{73, ID}, M. Planinic ⁸⁸, F. Pliquet ⁶³, M.G. Poghosyan ^{86, ID}, S. Politano ^{29, ID}, N. Poljak ^{88, ID}, A. Pop ^{45, ID}, S. Porteboeuf-Houssais ^{123, ID}, J. Porter ^{73, ID}, V. Pozdniakov ^{140, ID}, S.K. Prasad ^{4, ID}, S. Prasad ^{47, ID}, R. Preghenella ^{50, ID}, F. Prino ^{55, ID}, C.A. Pruneau ^{133, ID}, I. Pshenichnov ^{139, ID}, M. Puccio ^{32, ID}, S. Qiu ^{83, ID}, L. Quaglia ^{24, ID}, R.E. Quishpe ¹¹², S. Ragoni ^{99, ID}, A. Rakotozafindrabe ^{126, ID}, L. Ramello ^{129, 55, ID}, F. Rami ^{125, ID}, S.A.R. Ramirez ^{44, ID}, T.A. Rancien ⁷², R. Raniwala ^{91, ID}, S. Raniwala ⁹¹, S.S. Räsänen ^{43, ID}, R. Rath ^{47, ID}, I. Ravasenga ^{83, ID}, K.F. Read ^{86, 118, ID}, A.R. Redelbach ^{38, ID}, K. Redlich ^{78, ID, VI}, A. Rehman ²⁰, P. Reichelt ⁶³, F. Reidt ^{32, ID}, H.A. Reme-Ness ^{34, ID}, Z. Rescakova ³⁷, K. Reygers ^{94, ID}, A. Riabov ^{139, ID}, V. Riabov ^{139, ID}, R. Ricci ^{28, ID}, T. Richert ⁷⁴, M. Richter ^{19, ID}, W. Riegler ^{32, ID}, F. Riggi ^{26, ID}, C. Ristea ^{62, ID}, M. Rodríguez Cahuantzi ^{44, ID}, K. Røed ^{19, ID}, R. Rogalev ^{139, ID}, E. Rogochaya ^{140, ID}, T.S. Rogoschinski ^{63, ID}, D. Rohr ^{32, ID}, D. Röhrich ^{20, ID}, P.F. Rojas ⁴⁴, S. Rojas Torres ^{35, ID}, P.S. Rokita ^{132, ID}, F. Ronchetti ^{48, ID}, A. Rosano ^{30, 52, ID}, E.D. Rosas ⁶⁴, A. Rossi ^{53, ID}, A. Roy ^{47, ID}, P. Roy ⁹⁸, S. Roy ^{46, ID}, N. Rubini ^{25, ID}, D. Ruggiano ^{132, ID}, R. Rui ^{23, ID}, B. Rumyantsev ¹⁴⁰, P.G. Russek ^{2, ID}, R. Russo ^{83, ID}, A. Rustamov ^{80, ID}, E. Ryabinkin ^{139, ID}, Y. Ryabov ^{139, ID}, A. Rybicki ^{105, ID}, H. Rytkonen ^{113, ID}, W. Rzesz ^{132, ID}, O.A.M. Saarimaki ^{43, ID}, R. Sadek ^{102, ID}, S. Sadovsky ^{139, ID}, J. Saetre ^{20, ID}, K. Šafařík ^{35, ID}, S.K. Saha ^{131, ID}, S. Saha ^{79, ID}, B. Sahoo ^{46, ID}, P. Sahoo ⁴⁶, R. Sahoo ^{47, ID}, S. Sahoo ⁶⁰, D. Sahu ^{47, ID}, P.K. Sahu ^{60, ID}, J. Saini ^{131, ID}, K. Sajdakova ³⁷, S. Sakai ^{121, ID}, M.P. Salvan ^{97, ID}, S. Sambyal ^{90, ID}, T.B. Saramela ¹⁰⁸, D. Sarkar ^{133, ID}, N. Sarkar ¹³¹, P. Sarma ^{41, ID}, V. Sarritzu ^{22, ID}, V.M. Sarti ^{95, ID}, M.H.P. Sas ^{136, ID}, J. Schambach ^{86, ID}, H.S. Scheid ^{63, ID}, C. Schiaua ^{45, ID}, R. Schicker ^{94, ID}, A. Schmah ⁹⁴, C. Schmidt ^{97, ID}, H.R. Schmidt ⁹³, M.O. Schmidt ^{32, ID}, M. Schmidt ⁹³, N.V. Schmidt ^{86, 63, ID}, A.R. Schmier ^{118, ID}, R. Schotter ^{125, ID}, J. Schukraft ^{32, ID}, K. Schwarz ⁹⁷, K. Schweda ^{97, ID}, G. Scioli ^{25, ID}, E. Scomparin ^{55, ID}, J.E. Seger ^{14, ID}, Y. Sekiguchi ¹²⁰, D. Sekihata ^{120, ID}, I. Selyuzhenkov ^{97, 139, ID}, S. Senyukov ^{125, ID}, J.J. Seo ^{57, ID}, D. Serebryakov ^{139, ID}, L. Šerkšnytė ^{95, ID}, A. Sevcenco ^{62, ID}, T.J. Shaba ^{67, ID}, A. Shabanov ¹³⁹, A. Shabetai ^{102, ID}, R. Shahoyan ³², W. Shaikh ⁹⁸, A. Shangaraev ^{139, ID}, A. Sharma ⁸⁹, D. Sharma ^{46, ID}, H. Sharma ^{105, ID}, M. Sharma ^{90, ID}, N. Sharma ^{89, ID}, S. Sharma ^{90, ID}, U. Sharma ^{90, ID}, A. Shatat ^{127, ID}, O. Sheibani ¹¹², K. Shigaki ^{92, ID}, M. Shimomura ⁷⁶, S. Shirinkin ^{139, ID}, Q. Shou ^{39, ID}, Y. Sibirjak ^{139, ID}, S. Siddhanta ^{51, ID}, T. Siemiarczuk ^{78, ID}, T.F. Silva ^{108, ID}, D. Silvermyr ^{74, ID}, T. Simantathammakul ¹⁰³, R. Simeonov ^{36, ID}, G. Simonetti ³², B. Singh ⁹⁰, B. Singh ^{95, ID}, R. Singh ^{79, ID}, R. Singh ^{90, ID}, R. Singh ^{47, ID}, V.K. Singh ^{131, ID}, V. Singhal ^{131, ID}, T. Sinha ^{98, ID}, B. Sitar ^{12, ID}, M. Sitta ^{129, 55, ID}, T.B. Skaali ¹⁹, G. Skorodumovs ^{94, ID}, M. Slupecki ^{43, ID}, N. Smirnov ^{136, ID}, R.J.M. Snellings ^{58, ID}, E.H. Solheim ^{19, ID}, C. Soncco ¹⁰⁰, J. Song ^{112, ID}, A. Songmolnak ¹⁰³, F. Soramel ^{27, ID}, S.P. Sorensen ^{118, ID}, R. Soto Camacho ⁴⁴, R. Spijkers ^{83, ID}, I. Sputowska ^{105, ID}, J. Staa ^{74, ID}, J. Stachel ^{94, ID}, I. Stan ^{62, ID}, P.J. Steffanic ^{118, ID}, S.F. Stiefelmaier ^{94, ID}, D. Stocco ^{102, ID}, I. Storehaug ^{19, ID}, M.M. Storetvedt ^{34, ID}, P. Stratmann ^{134, ID}, S. Strazzi ^{25, ID}, C.P. Stylianidis ⁸³, A.A.P. Suáide ^{108, ID}, C. Suire ^{127, ID}, M. Sukhanov ^{139, ID}, M. Suljic ^{32, ID}, V. Sumberia ^{90, ID}, S. Sumowidagdo ^{81, ID}, S. Swain ⁶⁰, A. Szabo ¹², I. Szarka ^{12, ID}, U. Tabassam ¹³, S.F. Taghavi ^{95, ID}, G. Taillepied ^{97, 123, ID}, J. Takahashi ^{109, ID}, G.J. Tambave ^{20, ID}, S. Tang ^{123, 6, ID},

- Z. Tang ^{116, ID}, J.D. Tapia Takaki ^{114, ID}, N. Tapus ¹²², L.A. Tarasovicova ^{134, ID}, M. Tarhini ^{102, ID},
 M.G. Tarzila ^{45, ID}, A. Tauro ^{32, ID}, A. Telesca ^{32, ID}, L. Terlizzi ^{24, ID}, C. Terrevoli ^{112, ID}, G. Tersimonov ³,
 S. Thakur ^{131, ID}, D. Thomas ^{106, ID}, R. Tieulent ^{124, ID}, A. Tikhonov ^{139, ID}, A.R. Timmins ^{112, ID}, M. Tkacik ¹⁰⁴,
 T. Tkacik ^{104, ID}, A. Toia ^{63, ID}, N. Topilskaya ^{139, ID}, M. Toppi ^{48, ID}, F. Torales-Acosta ¹⁸, T. Tork ^{127, ID},
 A.G. Torres Ramos ^{31, ID}, A. Trifiró ^{30, 52, ID}, A.S. Triolo ^{30, 52, ID}, S. Tripathy ^{50, ID}, T. Tripathy ^{46, ID},
 S. Trogolo ^{32, ID}, V. Trubnikov ^{3, ID}, W.H. Trzaska ^{113, ID}, T.P. Trzcinski ^{132, ID}, R. Turrisi ^{53, ID}, T.S. Tveter ^{19, ID},
 K. Ullaland ^{20, ID}, B. Ulukutlu ^{95, ID}, A. Uras ^{124, ID}, M. Urioni ^{54, 130, ID}, G.L. Usai ^{22, ID}, M. Vala ³⁷,
 N. Valle ^{21, ID}, S. Vallero ^{55, ID}, L.V.R. van Doremalen ⁵⁸, M. van Leeuwen ^{83, ID}, C.A. van Veen ^{94, ID},
 R.J.G. van Weelden ^{83, ID}, P. Vande Vyvre ^{32, ID}, D. Varga ^{135, ID}, Z. Varga ^{135, ID}, M. Varga-Kofarago ^{135, ID},
 M. Vasileiou ^{77, ID}, A. Vasiliev ^{139, ID}, O. Vázquez Doce ^{95, ID}, O. Vazquez Rueda ^{74, ID}, V. Vechernin ^{139, ID},
 E. Vercellin ^{24, ID}, S. Vergara Limón ⁴⁴, L. Vermunt ^{58, ID}, R. Vértesi ^{135, ID}, M. Verweij ^{58, ID}, L. Vickovic ³³,
 Z. Vilakazi ¹¹⁹, O. Villalobos Baillie ^{99, ID}, G. Vino ^{49, ID}, A. Vinogradov ^{139, ID}, T. Virgili ^{28, ID}, V. Vislavicius ⁸²,
 A. Vodopyanov ^{140, ID}, B. Volkel ^{32, ID}, M.A. Völkl ^{94, ID}, K. Voloshin ¹³⁹, S.A. Voloshin ^{133, ID}, G. Volpe ^{31, ID},
 B. von Haller ^{32, ID}, I. Vorobyev ^{95, ID}, N. Vozniuk ^{139, ID}, J. Vrláková ^{37, ID}, B. Wagner ²⁰, C. Wang ^{39, ID},
 D. Wang ³⁹, M. Weber ^{101, ID}, A. Wegrzynek ^{32, ID}, F.T. Weiglhofer ³⁸, S.C. Wenzel ^{32, ID}, J.P. Wessels ^{134, ID},
 S.L. Weyhmiller ^{136, ID}, J. Wiechula ^{63, ID}, J. Wikne ^{19, ID}, G. Wilk ^{78, ID}, J. Wilkinson ^{97, ID}, G.A. Willems ^{134, ID},
 B. Windelband ^{94, ID}, M. Winn ^{126, ID}, J.R. Wright ^{106, ID}, W. Wu ³⁹, Y. Wu ^{116, ID}, R. Xu ^{6, ID}, A.K. Yadav ^{131, ID},
 S. Yalcin ^{71, ID}, Y. Yamaguchi ^{92, ID}, K. Yamakawa ⁹², S. Yang ²⁰, S. Yano ^{92, ID}, Z. Yin ^{6, ID}, I.-K. Yoo ^{16, ID},
 J.H. Yoon ^{57, ID}, S. Yuan ²⁰, A. Yuncu ^{94, ID}, V. Zaccolo ^{23, ID}, C. Zampolli ^{32, ID}, H.J.C. Zanolli ⁵⁸, F. Zanone ^{94, ID},
 N. Zardoshti ^{32, 99, ID}, A. Zarochentsev ^{139, ID}, P. Závada ^{61, ID}, N. Zaviyalov ¹³⁹, M. Zhalov ^{139, ID}, B. Zhang ^{6, ID},
 S. Zhang ^{39, ID}, X. Zhang ^{6, ID}, Y. Zhang ¹¹⁶, M. Zhao ^{10, ID}, V. Zherebchevskii ^{139, ID}, Y. Zhi ¹⁰,
 N. Zhigareva ¹³⁹, D. Zhou ^{6, ID}, Y. Zhou ^{82, ID}, J. Zhu ^{97, 6, ID}, Y. Zhu ⁶, G. Zinovjev ^{3, I}, N. Zurlo ^{130, 54, ID}

¹ A.I. Alikhanyan National Science Laboratory (Yerevan Physics Institute) Foundation, Yerevan, Armenia² AGH University of Krakow, Cracow, Poland³ Bogolyubov Institute for Theoretical Physics, National Academy of Sciences of Ukraine, Kiev, Ukraine⁴ Bose Institute, Department of Physics and Centre for Astroparticle Physics and Space Science (CAPSS), Kolkata, India⁵ California Polytechnic State University, San Luis Obispo, CA, United States⁶ Central China Normal University, Wuhan, China⁷ Centro de Aplicaciones Tecnológicas y Desarrollo Nuclear (CEADEN), Havana, Cuba⁸ Centro de Investigación y de Estudios Avanzados (CINVESTAV), Mexico City and Mérida, Mexico⁹ Chicago State University, Chicago, IL, United States¹⁰ China Institute of Atomic Energy, Beijing, China¹¹ Chungbuk National University, Cheongju, Republic of Korea¹² Comenius University Bratislava, Faculty of Mathematics, Physics and Informatics, Bratislava, Slovak Republic¹³ COMSATS University Islamabad, Islamabad, Pakistan¹⁴ Creighton University, Omaha, NE, United States¹⁵ Department of Physics, Aligarh Muslim University, Aligarh, India¹⁶ Department of Physics, Pusan National University, Pusan, Republic of Korea¹⁷ Department of Physics, Sejong University, Seoul, Republic of Korea¹⁸ Department of Physics, University of California, Berkeley, CA, United States¹⁹ Department of Physics, University of Oslo, Oslo, Norway²⁰ Department of Physics and Technology, University of Bergen, Bergen, Norway²¹ Dipartimento di Fisica, Università di Pavia, Pavia, Italy²² Dipartimento di Fisica dell'Università and Sezione INFN, Cagliari, Italy²³ Dipartimento di Fisica dell'Università and Sezione INFN, Trieste, Italy²⁴ Dipartimento di Fisica dell'Università and Sezione INFN, Turin, Italy²⁵ Dipartimento di Fisica e Astronomia dell'Università and Sezione INFN, Bologna, Italy²⁶ Dipartimento di Fisica e Astronomia dell'Università and Sezione INFN, Catania, Italy²⁷ Dipartimento di Fisica e Astronomia dell'Università and Sezione INFN, Padova, Italy²⁸ Dipartimento di Fisica 'E.R. Caianiello' dell'Università and Gruppo Collegato INFN, Salerno, Italy²⁹ Dipartimento DISAT del Politecnico and Sezione INFN, Turin, Italy³⁰ Dipartimento di Scienze MIFT, Università di Messina, Messina, Italy³¹ Dipartimento Interateneo di Fisica 'M. Merlin' and Sezione INFN, Bari, Italy³² European Organization for Nuclear Research (CERN), Geneva, Switzerland³³ Faculty of Electrical Engineering, Mechanical Engineering and Naval Architecture, University of Split, Split, Croatia³⁴ Faculty of Engineering and Science, Western Norway University of Applied Sciences, Bergen, Norway³⁵ Faculty of Nuclear Sciences and Physical Engineering, Czech Technical University in Prague, Prague, Czech Republic³⁶ Faculty of Physics, Sofia University, Sofia, Bulgaria³⁷ Faculty of Science, P.J. Šafárik University, Košice, Slovak Republic³⁸ Frankfurt Institute for Advanced Studies, Johann Wolfgang Goethe-Universität Frankfurt, Frankfurt, Germany

- ³⁹ Fudan University, Shanghai, China
⁴⁰ Gangneung-Wonju National University, Gangneung, Republic of Korea
⁴¹ Gauhati University, Department of Physics, Guwahati, India
⁴² Helmholtz-Institut für Strahlen- und Kernphysik, Rheinische Friedrich-Wilhelms-Universität Bonn, Bonn, Germany
⁴³ Helsinki Institute of Physics (HIP), Helsinki, Finland
⁴⁴ High Energy Physics Group, Universidad Autónoma de Puebla, Puebla, Mexico
⁴⁵ Horia Hulubei National Institute of Physics and Nuclear Engineering, Bucharest, Romania
⁴⁶ Indian Institute of Technology Bombay (IIT), Mumbai, India
⁴⁷ Indian Institute of Technology Indore, Indore, India
⁴⁸ INFN, Laboratori Nazionali di Frascati, Frascati, Italy
⁴⁹ INFN, Sezione di Bari, Bari, Italy
⁵⁰ INFN, Sezione di Bologna, Bologna, Italy
⁵¹ INFN, Sezione di Cagliari, Cagliari, Italy
⁵² INFN, Sezione di Catania, Catania, Italy
⁵³ INFN, Sezione di Padova, Padova, Italy
⁵⁴ INFN, Sezione di Pavia, Pavia, Italy
⁵⁵ INFN, Sezione di Torino, Turin, Italy
⁵⁶ INFN, Sezione di Trieste, Trieste, Italy
⁵⁷ Inha University, Incheon, Republic of Korea
⁵⁸ Institute for Gravitational and Subatomic Physics (GRASP), Utrecht University/Nikhef, Utrecht, Netherlands
⁵⁹ Institute of Experimental Physics, Slovak Academy of Sciences, Košice, Slovak Republic
⁶⁰ Institute of Physics, Homi Bhabha National Institute, Bhubaneswar, India
⁶¹ Institute of Physics of the Czech Academy of Sciences, Prague, Czech Republic
⁶² Institute of Space Science (ISS), Bucharest, Romania
⁶³ Institut für Kernphysik, Johann Wolfgang Goethe-Universität Frankfurt, Frankfurt, Germany
⁶⁴ Instituto de Ciencias Nucleares, Universidad Nacional Autónoma de México, Mexico City, Mexico
⁶⁵ Instituto de Física, Universidade Federal do Rio Grande do Sul (UFRGS), Porto Alegre, Brazil
⁶⁶ Instituto de Física, Universidad Nacional Autónoma de México, Mexico City, Mexico
⁶⁷ iThemba LABS, National Research Foundation, Somerset West, South Africa
⁶⁸ Jeonbuk National University, Jeonju, Republic of Korea
⁶⁹ Johann-Wolfgang-Goethe Universität Frankfurt Institut für Informatik, Fachbereich Informatik und Mathematik, Frankfurt, Germany
⁷⁰ Korea Institute of Science and Technology Information, Daejeon, Republic of Korea
⁷¹ KTO Karatay University, Konya, Turkey
⁷² Laboratoire de Physique Subatomique et de Cosmologie, Université Grenoble-Alpes, CNRS-IN2P3, Grenoble, France
⁷³ Lawrence Berkeley National Laboratory, Berkeley, CA, United States
⁷⁴ Lund University Department of Physics, Division of Particle Physics, Lund, Sweden
⁷⁵ Nagasaki Institute of Applied Science, Nagasaki, Japan
⁷⁶ Nara Women's University (NWU), Nara, Japan
⁷⁷ National and Kapodistrian University of Athens, School of Science, Department of Physics, Athens, Greece
⁷⁸ National Centre for Nuclear Research, Warsaw, Poland
⁷⁹ National Institute of Science Education and Research, Homi Bhabha National Institute, Jatni, India
⁸⁰ National Nuclear Research Center, Baku, Azerbaijan
⁸¹ National Research and Innovation Agency - BRIN, Jakarta, Indonesia
⁸² Niels Bohr Institute, University of Copenhagen, Copenhagen, Denmark
⁸³ Nikhef, National institute for subatomic physics, Amsterdam, Netherlands
⁸⁴ Nuclear Physics Group, STFC Daresbury Laboratory, Daresbury, United Kingdom
⁸⁵ Nuclear Physics Institute of the Czech Academy of Sciences, Husinec-Řež, Czech Republic
⁸⁶ Oak Ridge National Laboratory, Oak Ridge, TN, United States
⁸⁷ Ohio State University, Columbus, OH, United States
⁸⁸ Physics department, Faculty of science, University of Zagreb, Zagreb, Croatia
⁸⁹ Physics Department, Panjab University, Chandigarh, India
⁹⁰ Physics Department, University of Jammu, Jammu, India
⁹¹ Physics Department, University of Rajasthan, Jaipur, India
⁹² Physics Program and International Institute for Sustainability with Knotted Chiral Meta Matter (SKCM2), Hiroshima University, Hiroshima, Japan
⁹³ Physikalisches Institut, Eberhard-Karls-Universität Tübingen, Tübingen, Germany
⁹⁴ Physikalisches Institut, Ruprecht-Karls-Universität Heidelberg, Heidelberg, Germany
⁹⁵ Physik Department, Technische Universität München, Munich, Germany
⁹⁶ Politecnico di Bari and Sezione INFN, Bari, Italy
⁹⁷ Research Division and ExtreMe Matter Institute EMMI, GSI Helmholtzzentrum für Schwerionenforschung GmbH, Darmstadt, Germany
⁹⁸ Saha Institute of Nuclear Physics, Homi Bhabha National Institute, Kolkata, India
⁹⁹ School of Physics and Astronomy, University of Birmingham, Birmingham, United Kingdom
¹⁰⁰ Sección Física, Departamento de Ciencias, Pontificia Universidad Católica del Perú, Lima, Peru
¹⁰¹ Stefan Meyer Institut für Subatomare Physik (SMI), Vienna, Austria
¹⁰² SUBATECH, IMT Atlantique, Nantes Université, CNRS-IN2P3, Nantes, France
¹⁰³ Suranaree University of Technology, Nakhon Ratchasima, Thailand
¹⁰⁴ Technical University of Košice, Košice, Slovak Republic
¹⁰⁵ The Henryk Niewodniczanski Institute of Nuclear Physics, Polish Academy of Sciences, Cracow, Poland
¹⁰⁶ The University of Texas at Austin, Austin, TX, United States
¹⁰⁷ Universidad Autónoma de Sinaloa, Culiacán, Mexico
¹⁰⁸ Universidade de São Paulo (USP), São Paulo, Brazil
¹⁰⁹ Universidade Estadual de Campinas (UNICAMP), Campinas, Brazil
¹¹⁰ Universidade Federal do ABC, Santo André, Brazil
¹¹¹ University of Cape Town, Cape Town, South Africa
¹¹² University of Houston, Houston, TX, United States
¹¹³ University of Jyväskylä, Jyväskylä, Finland
¹¹⁴ University of Kansas, Lawrence, KS, United States
¹¹⁵ University of Liverpool, Liverpool, United Kingdom
¹¹⁶ University of Science and Technology of China, Hefei, China
¹¹⁷ University of South-Eastern Norway, Kongsberg, Norway
¹¹⁸ University of Tennessee, Knoxville, TN, United States

- ¹¹⁹ University of the Witwatersrand, Johannesburg, South Africa
¹²⁰ University of Tokyo, Tokyo, Japan
¹²¹ University of Tsukuba, Tsukuba, Japan
¹²² University Politehnica of Bucharest, Bucharest, Romania
¹²³ Université Clermont Auvergne, CNRS/IN2P3, LPC, Clermont-Ferrand, France
¹²⁴ Université de Lyon, CNRS/IN2P3, Institut de Physique des 2 Infinis de Lyon, Lyon, France
¹²⁵ Université de Strasbourg, CNRS, IPHC UMR 7178, F-67000 Strasbourg, France, Strasbourg, France
¹²⁶ Université Paris-Saclay, Centre d'Etudes de Saclay (CEA), IRFU, Département de Physique Nucléaire (DPhN), Saclay, France
¹²⁷ Université Paris-Saclay, CNRS/IN2P3, IJCLab, Orsay, France
¹²⁸ Università degli Studi di Foggia, Foggia, Italy
¹²⁹ Università del Piemonte Orientale, Vercelli, Italy
¹³⁰ Università di Brescia, Brescia, Italy
¹³¹ Variable Energy Cyclotron Centre, Homi Bhabha National Institute, Kolkata, India
¹³² Warsaw University of Technology, Warsaw, Poland
¹³³ Wayne State University, Detroit, MI, United States
¹³⁴ Westfälische Wilhelms-Universität Münster, Institut für Kernphysik, Münster, Germany
¹³⁵ Wigner Research Centre for Physics, Budapest, Hungary
¹³⁶ Yale University, New Haven, CT, United States
¹³⁷ Yonsei University, Seoul, Republic of Korea
¹³⁸ Zentrum für Technologie und Transfer (ZTT), Worms, Germany
¹³⁹ Affiliated with an institute covered by a cooperation agreement with CERN
¹⁴⁰ Affiliated with an international laboratory covered by a cooperation agreement with CERN

^I Deceased.

^{II} Also at: Max-Planck-Institut für Physik, Munich, Germany.

^{III} Also at: Italian National Agency for New Technologies, Energy and Sustainable Economic Development (ENEA), Bologna, Italy.

^{IV} Also at: Dipartimento DET del Politecnico di Torino, Turin, Italy.

^V Also at: Department of Applied Physics, Aligarh Muslim University, Aligarh, India.

^{VI} Also at: Institute of Theoretical Physics, University of Wroclaw, Poland.

^{VII} Also at: An institution covered by a cooperation agreement with CERN.